

Volume 19, Number 2/May 1981  
Published by the MIT Press  
ISSN 0028-3967

# NEUROSCIENCES

## Research Program Bulletin®

The F.O. Schmitt Lecture in Neuroscience 1980

THE RELATIONSHIP BETWEEN FUNCTION  
AND ENERGY METABOLISM:  
ITS USE IN THE LOCALIZATION  
OF FUNCTIONAL ACTIVITY  
IN THE NERVOUS SYSTEM

Louis Sokoloff

## NEUROSCIENCES RESEARCH PROGRAM

165 Allandale Street, Jamaica Plain Station, Boston, MA 02130

Telephone: (617) 522-6700 Cable: NEUROCENT

The Neurosciences Research Program, a research center of the Massachusetts Institute of Technology, is an interdisciplinary, interuniversity organization with the primary goal of facilitating the investigation of how the nervous system mediates behavior including the mental processes of man. To this end, the NRP, as one of its activities, conducts scientific meetings to explore the crucial problems in the neurosciences and publishes reports of these Work Sessions in the *Neurosciences Research Program Bulletin*. NRP is supported in part through Massachusetts Institute of Technology by National Institute of Mental Health Grant No. MH23132, National Institute of Neurological and Communicative Disorders and Stroke Grant NS15690, and Max-Planck-Gesellschaft, and through the Neurosciences Research Foundation by The Camille and Henry Dreyfus Foundation, Inc., The Beverly and Harvey Karp Foundation, van Ameringen Foundation, Inc., the G. Unger Vetlesen Foundation, and Vollmer Foundation, Inc.

*Director* Frederic G. Worden  
*Program Director* Lauren K. Gerbrandt

*Foundation Scientist* Francis O. Schmitt

*Staff Scientists* Stephanie J. Bird, Lawrence J. Mononen, Fred E. Samson • *Associate Director for Administration and Finance* Katheryn Cusick • *Editor and Librarian* George Adelman • *Publications Coordinator* Yvonne M. Homsy

---

The *Neurosciences Research Program Bulletin* is published by the MIT Press Journals, Cambridge, Massachusetts, and London, England, and is sold on a volume basis only. Subscriptions are \$60.00 per volume for institutions, \$40.00 for individuals for personal use, and \$30.00 for students. Prices are subject to change without notice. (Foreign subscribers, excluding those in Canada and PUAS, please add \$3.00 for additional postage.) For information on the availability of back issues and other publications of NRP, see back pages.

Second class postage paid at Boston, MA and at additional mailing offices. The *Neuroresearch Program Bulletin* is published four times yearly, in February, June, September and December.

Subscription correspondence should be addressed to NRP Bulletin. The MIT Press, 28 Carleton Street, Cambridge, Massachusetts 02142. Claims for missing issues must be made on or before receipt of the next published issue. Please notify the MIT Press six to eight weeks in advance of any change of address to ensure proper delivery of the Bulletin. Where possible, include address label. Postmaster: Send address changes to Neurosciences Research Program Bulletin, 28 Carleton Street, Cambridge, MA 02142.

© 1981 by the Massachusetts Institute of Technology

THE F.O. SCHMITT LECTURE IN NEUROSCIENCE 1980

THE RELATIONSHIP BETWEEN FUNCTION AND  
ENERGY METABOLISM: ITS USE IN THE  
LOCALIZATION OF FUNCTIONAL ACTIVITY  
IN THE NERVOUS SYSTEM

Louis Sokoloff  
National Institute of Mental Health  
Bethesda, Maryland

Louis Sokoloff is Chief of the Laboratory of Cerebral Metabolism of the National Institute of Mental Health, Bethesda, Maryland.

This text is based in part on the author's F.O. Schmitt Lecture in Neuroscience, delivered at Kresge Auditorium, Massachusetts Institute of Technology, March 18, 1980. It was the seventh in this series of lectures.

## FOREWORD

The F.O. Schmitt Lecture and Prize in Neuroscience was established by the Associates of the Neurosciences Research Program in 1973 to mark the seventeenth birthday of Francis O. Schmitt, founder of the organization. The purpose of the award is to recognize, encourage, and advance the achievement of excellence in neuroscience.

John Z. Young was the first recipient of the award and subsequent awardees have been Solomon H. Snyder and Leslie Iversen, Vernon B. Mountcastle, Victor Hamburger, Roger Guillemin, and Stephen W. Kuffler.

Louis Sokoloff received the F.O. Schmitt Prize for 1980 in recognition of his contributions to neurochemistry and cerebral physiology. The Prize was presented with the following citation:

“For his synthesis of neurochemistry, enzyme kinetics, and circulatory physiology in the development of techniques to quantitate cerebral metabolism and cerebral blood flow; for his use of these techniques to demonstrate the relations between glucose utilization and the functional activity of the brain and, in particular, to elucidate brain mechanisms of visual information processing, of psychotropic drug action, and of circadian rhythmicity; for his catalytic contributions to the work of other neuroscientists in their applications of his discoveries in clinical determinations of cerebral blood flow and metabolism by positron emission tomography; and for his pioneering work, which helped develop the field of modern neurochemistry.”

## INTRODUCTION

The brain is a complex, heterogeneous organ composed of many anatomical and functional components with markedly different levels of activity that vary independently with time and function. Other tissues are generally far more homogeneous, with most of their cells acting similarly and synchronously in response to a common stimulus or regulatory influence. The central nervous system, however, consists of innumerable subunits, each integrated into its own set of functional pathways and networks and subserving only one or a few of the many activities in which the nervous system participates. Understanding how the nervous system functions requires knowledge not only of the mechanisms of excitation and inhibition but even more so of their precise localization in the nervous system and the relationships of neural subunits to specific functions.

Historically, studies of the central nervous system have concentrated heavily on localization of function and mapping of pathways related to specific functions. These have been carried out neuroanatomically and histologically with staining and degeneration techniques, behaviorally with ablation and stimulation techniques, electrophysiologically with electrical recording and evoked electrical responses, and histochemically with a variety of techniques, including fluorescent and immunofluorescent methods and autoradiography of orthograde and retrograde axoplasmic flow. Many of these conventional methods suffer from a sampling problem. They generally permit examination of only one potential pathway at a time, and only positive results are interpretable. Furthermore, the demonstration of a pathway reveals only a potential for function; it does not reveal its significance in normal function.

Tissues that do physical and/or chemical work, such as heart, kidney, and skeletal muscle, exhibit a close relationship between energy metabolism and functional activity. From measurement of energy metabolism it is then possible to estimate the level of functional activity. The existence of a similar relationship in the tissues of the central nervous system has been more difficult to prove, partly because of uncertainty about the nature of the work associated with nervous functional activity, but mainly because of the difficulty in assessing the levels of functional and metabolic activities in the same functional component of the brain at the same time. Much of our present knowledge of cerebral energy metabolism *in vivo* has been obtained by means of the nitrous oxide technique of Kety and Schmidt (1948a) and its modifications (Scheinberg and Stead, 1949; Lassen and Munck, 1955; Eklöf et al., 1973; Gjedde et al., 1975), which measure the average

rates of energy metabolism in the brain as a whole. These methods have demonstrated changes in cerebral metabolic rate in association with gross or diffuse alterations of cerebral function and/or structure, as, for example, those that occur during postnatal development, aging, senility, anesthesia, disorders of consciousness, and convulsive states (Kety, 1950, 1957; Lassen, 1959; Sokoloff, 1960, 1976). They have not detected changes in cerebral metabolic rate in a number of conditions with, perhaps, more subtle alterations in cerebral functional activity; for example, deep slow-wave sleep, performance of mental arithmetic, sedation and tranquilization, schizophrenia, and LSD-induced psychosis (Kety, 1950; Lassen, 1959; Sokoloff, 1969). It is possible that there are no changes in cerebral energy metabolism in these conditions. The apparent lack of change could also be explained by either a redistribution of local levels of functional and metabolic activity without significant change in the average of the brain as a whole or the restriction of altered metabolic activity to regions too small to be detected in measurements of the brain as a whole. What has clearly been needed is a method that measures the rates of energy metabolism in specific discrete regions of the brain in normal and altered states of functional activity.

Kety and his associates (Landau et al., 1955; Freygang and Sokoloff, 1958; Kety, 1960; Reivich et al., 1969) developed a quantitative autoradiographic technique to measure the local tissue concentrations of chemically inert, diffusible, radioactive tracers that they used to determine the rates of blood flow simultaneously in all the structural components visible and identifiable in autoradiographs of serial sections of the brain. The application of this quantitative autoradiographic technique to the determination of local cerebral metabolic rate has proved to be more difficult because of the inherently greater complexity of the problem and the unsuitability of the labeled species of the normal substrates of cerebral energy metabolism, oxygen and glucose. The radioisotopes of oxygen have too short a physical half-life. Both oxygen and glucose are too rapidly converted to carbon dioxide, and  $\text{CO}_2$  is too rapidly cleared from the cerebral tissues. Sacks (1957), for example, has found in man significant losses of  $^{14}\text{CO}_2$  from the brain within two minutes after the onset of an intravenous infusion of [ $^{14}\text{C}$ ] glucose, labeled either uniformly, in the C-1, C-2, or C-6 positions. These limitations of [ $^{14}\text{C}$ ] glucose have been avoided by the use of 2-deoxy-D-[ $^{14}\text{C}$ ] glucose, a labeled analogue of glucose with special properties that make it particularly appropriate for this application (Sokoloff et al., 1977). It is metabolized through part of the pathway of glucose metabolism at a definable rate relative to that of glucose. Unlike glucose, however, its product, [ $^{14}\text{C}$ ] deoxyglucose-6-phosphate,

is essentially trapped in the tissues, allowing the application of the quantitative autoradiographic technique. The use of radioactive 2-deoxyglucose (DG) to trace glucose utilization and the autoradiographic technique to achieve regional localization has recently led to the development of a method that measures the rates of glucose utilization simultaneously in all components of the central nervous system in the normal conscious state and during experimental physiological, pharmacological, and pathological conditions (Sokoloff et al., 1977). Because the procedure is so designed that the concentrations of radioactivity in the tissues during autoradiography are more or less proportional to the rates of glucose utilization, the autoradiographs provide pictorial representations of the relative rates of glucose utilization in all the cerebral structures visualized. Numerous studies with this method have established that there is a close relationship between functional activity and energy metabolism in the central nervous system (Sokoloff, 1977; Plum et al., 1976), and the method has become a potent new tool for mapping functional neural pathways on the basis of evoked metabolic responses.

## THEORY

The method is derived from a model based on the biochemical properties of 2-deoxyglucose (Figure 1) (Sokoloff et al., 1977). DG is transported bidirectionally between blood and brain by the same carrier that transports glucose across the blood-brain barrier (Bidder, 1968; Bachelard, 1971; Oldendorf, 1971). In the cerebral tissues it is phosphorylated by hexokinase to 2-deoxyglucose-6-phosphate (DG-6-P) (Sols and Crane, 1954). Deoxyglucose and glucose are, therefore, competitive substrates for both blood-brain transport and hexokinase-catalyzed phosphorylation. Unlike glucose-6-phosphate (G-6-P), however, which is metabolized further eventually to CO<sub>2</sub> and water and to a lesser degree via the hexosemonophosphate shunt, DG-6-P cannot be converted to fructose-6-phosphate and is not a substrate for G-6-P dehydrogenase (Sols and Crane, 1954). There is very little glucose-6-phosphatase activity in brain (Hers, 1957) and even less deoxyglucose-6-phosphatase activity (Sokoloff et al., 1977). Deoxyglucose-6-phosphate, once formed, is, therefore, essentially trapped in the cerebral tissues, at least long enough for the duration of the measurement. The half-lives of [<sup>14</sup>C]deoxyglucose-6-phosphate in the various cerebral tissues have been experimentally estimated; the average half-lives are 7.7 (S.D. = ± 1.6) and 9.7 (S.D. = ± 2.6) hours in gray and white matter, respectively (Sokoloff et al., 1977). The shortest half-life is 6.1 hours in the inferior colliculus (Sokoloff et al., 1977).

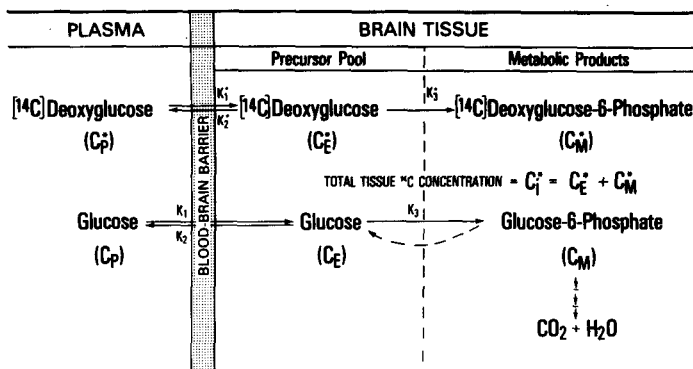


Figure 1.

Diagrammatic representation of the theoretical model.  $C_t^*$  represents the total  $^{14}\text{C}$  concentration in a single homogeneous tissue of the brain.  $C_p^*$  and  $C_p$  represent the concentrations of  $[^{14}\text{C}]$ deoxyglucose and glucose, respectively, in the arterial plasma;  $C_E^*$  and  $C_E$  represent their respective concentrations in the tissue pools that serve as substrates for hexokinase.  $C_M^*$  represents the concentration of  $[^{14}\text{C}]$ deoxyglucose-6-phosphate in the tissue. The constants  $k_1^*$ ,  $k_2^*$ , and  $k_3^*$ , represent the rate constants for carrier-mediated transport of  $[^{14}\text{C}]$ -deoxyglucose from plasma to tissue, for carrier-mediated transport back from tissue to plasma, and for phosphorylation by hexokinase, respectively. The constants  $k_1$ ,  $k_2$ , and  $k_3$  are the equivalent rate constants for glucose.  $[^{14}\text{C}]$ Deoxyglucose and glucose share and compete for the carrier that transports both between plasma and tissue and for hexokinase, which phosphorylates them to their respective hexose-6-phosphates. The dashed arrow represents the possibility of glucose-6-phosphate hydrolysis by glucose-6-phosphatase activity, if any. [Sokoloff et al., 1977]

If the interval of time is kept short enough, for example less than one hour, to allow the assumption of negligible loss of  $[^{14}\text{C}]$ DG-6-P from the tissues, then the quantity of  $[^{14}\text{C}]$ DG-6-P accumulated in any cerebral tissue at any given time following the introduction of  $[^{14}\text{C}]$ DG into the circulation is equal to the integral of the rate of  $[^{14}\text{C}]$ DG phosphorylation by hexokinase in that tissue during that interval of time. This integral is in turn related to the amount of glucose that has been phosphorylated over the same interval, depending on the time courses of the relative concentrations of  $[^{14}\text{C}]$ DG and glucose in the precursor pools and the Michaelis-Menten kinetic constants for hexokinase with respect to both  $[^{14}\text{C}]$ DG and glucose. With cerebral glucose consumption in a steady state, the amount of glucose phosphorylated during the interval of time equals the steady state flux of glucose through the hexokinase-catalyzed step times the duration of the interval, and the net rate of flux of glucose through this step equals the rate of glucose utilization.

These relationships can be mathematically defined and an operational equation derived if the following assumptions are made: (1) a steady state for glucose (i.e., constant plasma glucose concentration and constant rate of glucose consumption) throughout the period of

the procedure; (2) homogeneous tissue compartment within which the concentrations of [<sup>14</sup>C] DG and glucose are uniform and exchange directly with the plasma; and (3) tracer concentrations of [<sup>14</sup>C] DG (i.e., molecular concentrations of free [<sup>14</sup>C] DG essentially equal to zero). The operational equation that defines  $R_i$ , the rate of glucose consumption per unit mass of tissue,  $i$ , in terms of measurable variables is presented in Figure 2.

The rate constants are determined in a separate group of animals by a nonlinear, iterative process. This process provides the least squares best-fit of an equation that defines the time course of total tissue <sup>14</sup>C concentration in terms of the time, the history of the plasma concentration, and the rate constants to the experimentally determined time courses of tissue and plasma concentrations of <sup>14</sup>C

General Equation for Measurement of Reaction Rates with Tracers:

$$\text{Rate of Reaction} = \frac{\text{Labeled Product Formed in Interval of Time, 0 to T}}{\left[ \begin{array}{c} \text{Isotope Effect} \\ \text{Correction Factor} \end{array} \right] \left[ \begin{array}{c} \text{Integrated Specific Activity} \\ \text{of Precursor} \end{array} \right]}$$

Operational Equation of [<sup>14</sup>C]Deoxyglucose Method:

$$R_i = \frac{\overbrace{\text{Total } ^{14}\text{C in Tissue at Time, T}}^{\text{Labeled Product Formed in Interval of Time, 0 to T}} - \overbrace{k_T^* e^{-(k_2^* + k_3^*)T} \int_0^T C_p^* e^{(k_2^* + k_3^*)t} dt}^{\text{ } ^{14}\text{C in Precursor Remaining in Tissue at Time, T}}}{\underbrace{\left[ \frac{\lambda \cdot V_m^* \cdot K_m}{\Phi \cdot V_m \cdot K_m^*} \right]}_{\text{Isotope Effect Correction Factor}} \left[ \underbrace{\int_0^T \left( \frac{C_p^*}{C_p} \right) dt}_{\text{Integrated Plasma Specific Activity}} - \underbrace{e^{-(k_2^* + k_3^*)T} \int_0^T \left( \frac{C_p^*}{C_p} \right) e^{(k_2^* + k_3^*)t} dt}_{\text{Correction for Lag in Tissue Equilibration with Plasma}} \right]}_{\text{Integrated Precursor Specific Activity in Tissue}}$$

Figure 2.

Operational equation of radioactive deoxyglucose method and its functional anatomy.  $T$  represents the time at the termination of the experimental period;  $\lambda$  equals the ratio of the distribution space of deoxyglucose in the tissue to that of glucose;  $\Phi$  equals the fraction of glucose that, once phosphorylated, continues down the glycolytic pathway; and  $k_m^*$  and  $V_m^*$  and  $K_m$  and  $V_m$  represent the familiar Michaelis-Menten kinetic constants of hexokinase for deoxyglucose and glucose, respectively. The other symbols are the same as those defined in Figure 1. [Sokoloff, 1978]

**Table 1**  
 Values of Rate Constants in the Normal Conscious Albino Rat [Sokoloff et al., 1977]

Structure	Rate constants (min <sup>-1</sup> )			Distribution volume (ml/g)	Half-life of precursor pool (min)
	$k_1^*$	$k_2^*$	$k_3^*$	$k_1^*/(k_2^* + k_3^*)$	$\text{Log}_e 2 / (k_2^* + k_3^*)$
<b>Gray matter</b>					
Visual cortex	0.189 ± 0.048	0.279 ± 0.176	0.063 ± 0.040	0.553	2.03
Auditory cortex	0.226 ± 0.068	0.241 ± 0.198	0.067 ± 0.057	0.734	2.25
Parietal cortex	0.194 ± 0.051	0.257 ± 0.175	0.062 ± 0.045	0.608	2.17
Sensory-motor cortex	0.193 ± 0.037	0.208 ± 0.112	0.049 ± 0.035	0.751	2.70
Thalamus	0.188 ± 0.045	0.218 ± 0.144	0.053 ± 0.043	0.694	2.56
Medial geniculate body	0.219 ± 0.055	0.259 ± 0.164	0.055 ± 0.040	0.697	2.21
Lateral geniculate body	0.172 ± 0.038	0.220 ± 0.134	0.055 ± 0.040	0.625	2.52
Hypothalamus	0.158 ± 0.032	0.266 ± 0.119	0.043 ± 0.032	0.587	2.58
Hippocampus	0.169 ± 0.043	0.260 ± 0.166	0.056 ± 0.040	0.535	2.19
Amygdala	0.149 ± 0.028	0.235 ± 0.109	0.032 ± 0.026	0.558	2.60
Caudate-putamen	0.176 ± 0.041	0.200 ± 0.140	0.061 ± 0.050	0.674	2.66
Superior colliculus	0.198 ± 0.054	0.240 ± 0.166	0.046 ± 0.042	0.692	2.42
Pontine gray matter	0.170 ± 0.040	0.246 ± 0.142	0.037 ± 0.033	0.601	2.45
Cerebellar cortex	0.225 ± 0.066	0.392 ± 0.229	0.059 ± 0.031	0.499	1.54
Cerebellar nucleus	0.207 ± 0.042	0.194 ± 0.111	0.038 ± 0.035	0.892	2.99
Mean ± S.E.M.	0.189 ± 0.012	0.245 ± 0.040	0.052 ± 0.010	0.647 ± 0.073	2.39 ± 0.40
<b>White matter</b>					
Corpus callosum	0.085 ± 0.015	0.135 ± 0.075	0.019 ± 0.033	0.552	4.50
Genu of corpus callosum	0.076 ± 0.013	0.131 ± 0.075	0.019 ± 0.034	0.507	4.62
Internal capsule	0.077 ± 0.015	0.134 ± 0.085	0.023 ± 0.039	0.490	4.41
Mean ± S.E.M.	0.079 ± 0.008	0.133 ± 0.046	0.020 ± 0.020	0.516 ± 0.171	4.51 ± 0.90

(Sokoloff et al., 1977). The rate constants have thus far been completely determined only in normal, conscious albino rats (Table 1). Partial analyses indicate that the values are quite similar in the conscious monkey (Kennedy et al., 1978).

The  $\lambda$ ,  $\Phi$ , and the enzyme kinetic constants are grouped together to constitute a single, lumped constant (Figure 2). It can be shown mathematically that this lumped constant is equal to the asymptotic value of the product of the ratio of the cerebral extraction ratios of [ $^{14}\text{C}$ ]DG and glucose and the ratio of the arterial blood to plasma specific activities when the arterial plasma [ $^{14}\text{C}$ ]DG concentration is maintained constant (Sokoloff et al., 1977). The lumped constant is also determined in a separate group of animals from arterial and venous cerebral blood samples drawn during a programmed intravenous infusion that produces and maintains a constant arterial plasma [ $^{14}\text{C}$ ]DG concentration (Sokoloff et al., 1977). An example of such a determination in a conscious monkey is illustrated in Figure 3. Thus far the lumped constant has been determined only in the albino rat, monkey, cat, and dog (Table 2). The lumped constant appears to be characteristic of the species and does not appear to change significantly in a wide range of physiological conditions (Table 2) (Sokoloff et al., 1977).

Despite its complex appearance, the operational equation is really nothing more than a general statement of the standard relationship by which rates of enzyme-catalyzed reactions are determined from measurements made with radioactive tracers (Figure 2). The numerator of the equation represents the amount of radioactive product formed in a given interval of time; it is equal to  $C_i^*$ , the combined concentrations of [ $^{14}\text{C}$ ]DG and [ $^{14}\text{C}$ ]DG-6-P in the tissue at time,  $T$ , measured by the quantitative autoradiographic technique, less a term that represents the free unmetabolized [ $^{14}\text{C}$ ]DG still remaining in the tissue. The denominator represents the integrated specific activity of the precursor pool times a factor, the lumped constant, which is equivalent to a correction factor for an isotope effect. The term with the exponential factor in the denominator takes into the account the lag in the equilibration of the tissue precursor pool with the plasma.

## EXPERIMENTAL PROCEDURE FOR MEASUREMENT OF LOCAL CEREBRAL GLUCOSE UTILIZATION

### Theoretical Considerations in the Design of the Procedure

The operational equation of the method specifies the variables to be measured in order to determine  $R_i$ , the local rate of glucose con-

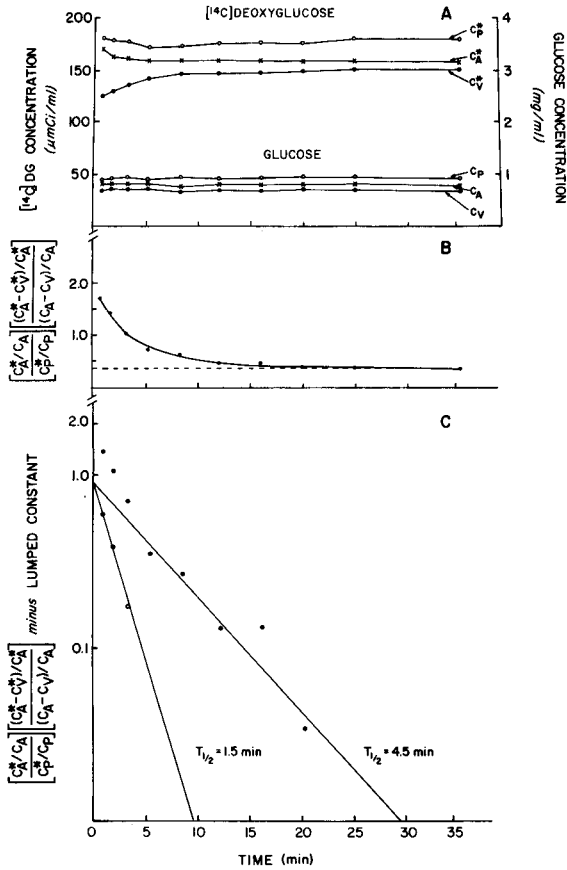


**Figure 3.**

Data obtained and their use in determination of the lumped constant and the combination of rate constants,  $(k_2^* + k_3^*)$ , in a representative experiment. A. Time courses of arterial blood and plasma concentrations of [<sup>14</sup>C] DG and glucose and cerebral venous blood concentrations of [<sup>14</sup>C] DG and glucose during programmed intravenous infusion of [<sup>14</sup>C] DG. B. Arithmetic plot of the function derived from the variables in A and combined as indicated in the formula on the ordinate against time. This function declines exponentially, with a rate constant equal to  $(k_2^* + k_3^*)$ , until it reaches an asymptotic value equal to the lumped constant, 0.35, in this experiment (dashed line). C. Semilogarithmic plot of the curve in B less the lumped constant, i.e., its asymptotic value. Solid circles represent actual values. This curve is analyzed into two components by a standard curve-peeling technique to yield the two straight lines representing the separate components. Open circles are points for the fast component, obtained by subtracting the values for the slow component from the solid circles. The rate constants for these two components represent the values of  $(k_2^* + k_3^*)$  for two compartments; the fast and slow compartments are assumed to represent gray and white matter, respectively. In this experiment the values for  $(k_2^* + k_3^*)$  were found to equal 0.462 (half-time = 1.5 min) and 0.154 (half-time = 4.5 min) in gray and white matter, respectively. [Kennedy et al., 1978]

**Table 2**

Values of the Lumped Constant in the Albino Rat, Rhesus Monkey, Cat, and Dog [Sokoloff, 1979]

Animal	No. of animals	Mean $\pm$ S.D.	S.E.M.
<b>Albino rat:</b>			
Conscious	15	0.464 $\pm$ 0.099*	$\pm$ 0.026
Anesthetized	9	0.512 $\pm$ 0.118*	$\pm$ 0.039
Conscious (5% CO <sub>2</sub> )	2	0.463 $\pm$ 0.122*	$\pm$ 0.086
Combined	26	0.481 $\pm$ 0.119	$\pm$ 0.023
<b>Rhesus monkey:</b>			
Conscious	7	0.344 $\pm$ 0.095	$\pm$ 0.036
<b>Cat:</b>			
Anesthetized	6	0.411 $\pm$ 0.013	$\pm$ 0.005
<b>Dog (beagle puppy):</b>			
Conscious	7	0.558 $\pm$ 0.082	$\pm$ 0.031

\*No statistically significant difference between normal conscious and anesthetized rats ( $0.3 < p < 0.4$ ) and conscious rats breathing 5% CO<sub>2</sub> ( $p > 0.9$ ).

The values were obtained as follows: rat, Sokoloff et al., 1977; monkey, Kennedy et al., 1978; cat, (M. Miyaoka, J. Magnes, C. Kennedy, M. Shinohara, and L. Sokoloff, unpublished data); dog, Duffy et al., 1979.

sumption in the brain. The following variables are measured in each experiment: (1) the entire history of the arterial plasma [<sup>14</sup>C]deoxyglucose concentration,  $C_p^*$ , from zero time to the time of killing,  $T$ ; (2) the steady-state arterial plasma glucose level,  $C_p$ , over the same interval; and (3) the local concentration of <sup>14</sup>C in the tissue at the time of killing,  $C_i^*(T)$ . The rate constants,  $k_1^*$ ,  $k_2^*$ , and  $k_3^*$ , and the lumped constant,  $\lambda V_m^* K_m / \Phi V_m K_m^*$ , are not measured in each experiment; the values for these constants that are used are those determined separately in other groups of animals, as described above and presented in Tables 1 and 2.

The operational equation is generally applicable with all types of arterial plasma [<sup>14</sup>C]DG concentration curves. Its configuration, however, suggests that a declining curve, approaching zero by the time of killing, is the choice to minimize certain potential errors. The quantitative autoradiographic technique measures only total <sup>14</sup>C concentration in the tissue and does not distinguish between [<sup>14</sup>C]DG-6-P and [<sup>14</sup>C]DG. It is, however, [<sup>14</sup>C]DG-6-P concentration that must be known to determine glucose consumption. [<sup>14</sup>C]DG-6-P concentration is calculated in the numerator of the operational equation, which equals the total tissue <sup>14</sup>C content,  $C_i^*(T)$ , minus

the [ $^{14}\text{C}$ ]DG concentration present in the tissue, estimated by the term containing the exponential factor and rate constants. In the denominator of the operational equation there is also a term containing an exponential factor and rate constants. Both these terms have the useful property of approaching zero with increasing time if  $C_p^*$  is also allowed to approach zero. The rate constants,  $k_1^*$ ,  $k_2^*$ , and  $k_3^*$ , are not measured in the same animals in which local glucose consumption is being measured. It is conceivable that the rate constants in Table 1 are not equally applicable in all physiological, pharmacological, and pathological states. One possible solution is to determine the rate constants for each condition to be studied. An alternative solution, and the one chosen, is to administer the [ $^{14}\text{C}$ ]DG as a single intravenous pulse at zero time and to allow sufficient time for the clearance of [ $^{14}\text{C}$ ]DG from the plasma and the terms containing the rate constants to fall to levels too low to influence the final result. To wait until these terms reach zero is impractical because of the long time required and the risk of effects of the small but finite rate of loss of [ $^{14}\text{C}$ ]DG-6-P from the tissues. A reasonable time interval is 45 minutes; by this time the plasma level has fallen to very low levels, and, on the basis of the values of  $(k_2^* + k_3^*)$  in Table 1, the exponential factors have declined through at least ten half-lives.

The time courses of the concentrations of [ $^{14}\text{C}$ ]DG and [ $^{14}\text{C}$ ]DG-6-P in arterial plasma and representative gray and white matter following an intravenous pulse of [ $^{14}\text{C}$ ]DG are illustrated in Figure 4. As the plasma concentration falls from its peak following the pulse, the tissue concentrations of [ $^{14}\text{C}$ ]DG first rise until the tissues and plasma reach equilibrium. As the plasma concentration continues to fall below its equilibrium levels, there is a net loss of [ $^{14}\text{C}$ ]DG back to the plasma, as well as continued conversion of tissue [ $^{14}\text{C}$ ]DG to [ $^{14}\text{C}$ ]DG-6-P, and the concentrations of free [ $^{14}\text{C}$ ]DG in the tissues then decline (Figure 4A). The higher the blood flow of the tissue, the more rapidly it initially takes up [ $^{14}\text{C}$ ]DG, but it reaches equilibrium with plasma sooner and loses [ $^{14}\text{C}$ ]DG more rapidly after the point of equilibrium. These opposing effects of blood flow before and after equilibrium tend to cancel out the effects of blood flow. By 45 minutes the tissue and plasma levels of free [ $^{14}\text{C}$ ]DG have reached very low levels. On the other hand, the [ $^{14}\text{C}$ ]DG-6-P concentrations in the tissues rise continuously and by 45 minutes are responsible for most of the  $^{14}\text{C}$  in the tissues, particularly in gray matter (Figure 4A). The numerator of the operational equation represents the final total tissue  $^{14}\text{C}$  concentration, measured autoradiographically, minus the final point on the tissue [ $^{14}\text{C}$ ]DG curve and is equal, therefore, to the final [ $^{14}\text{C}$ ]DG-6-P concentration in the tissue (Figure 4A).

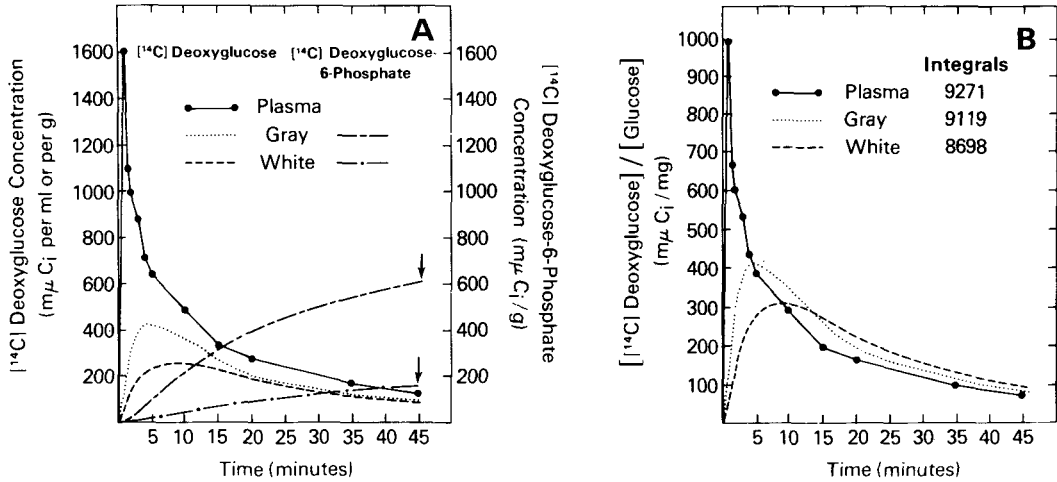


**Figure 4.**

Graphical representation of the significant variables in the operational equation used to calculate local cerebral glucose utilization. A. Time courses of [ $^{14}\text{C}$ ] DG concentrations in arterial plasma and in average gray and white matter and [ $^{14}\text{C}$ ] DG-6-P concentrations in average gray and white matter following an intravenous pulse of  $50 \mu\text{Ci}$  of [ $^{14}\text{C}$ ] deoxyglucose. The plasma curve is derived from measurements of plasma [ $^{14}\text{C}$ ] DG concentration. The tissue concentrations were calculated from the plasma curve and the mean values of  $k_1^*$ ,  $k_2^*$ , and  $k_3^*$  for gray and white matter in Table 1 according to the second term in the numerator of the operational equation. The [ $^{14}\text{C}$ ] DG-6-P concentrations in the tissues were calculated from the same variables by integration of the product of  $k_3^*$  and the tissue concentration of [ $^{14}\text{C}$ ] DG. The arrows point to the concentrations of [ $^{14}\text{C}$ ] DG and [ $^{14}\text{C}$ ] DG-6-P in the tissues at the time of killing; the autoradiographic technique measures the total  $^{14}\text{C}$  content (i.e., the sum of these concentrations) at that time, which is equal to  $C_i^*(T)$ , the first term in the numerator of the operational equation. Note that at the time of killing, the total  $^{14}\text{C}$  content represents mainly [ $^{14}\text{C}$ ] deoxyglucose-6-phosphate concentration, especially in gray matter. B. Time courses of ratios of [ $^{14}\text{C}$ ] deoxyglucose to glucose concentrations (i.e., specific activities) in plasma and average gray and white matter. The curve for plasma was determined by division of the plasma curve in (A) by the plasma glucose concentrations. The curves for the tissues were calculated by differentiation of the function in brackets in the denominator of the operational equation. The integrals in (B) are the integrals of the specific activities with respect to time and represent the areas under the curves. The integrals under the tissue curves are equivalent to all of the denominator of the operational equation, except for the lumped constant. Note that by the time of killing, the integrals of the tissue curves approach equality with each other and with that of the plasma curve. [Sokoloff et al., 1977]

The physical significance of the denominator of the operational equation is illustrated in Figure 4B. The curves in Figure 4B are derived from the curves for [ $^{14}\text{C}$ ]DG concentration in plasma and average gray and white matter in Figure 4A by dividing them by the glucose concentrations in those tissues. They represent, in effect, the time courses of the specific activities in those tissues. The integrals in Figure 4B are the integrated specific activities, i.e., the areas under each of the curves between zero and 45 minutes. The denominator of the operational equation is equal to the product of the lumped constant and the integral appropriate to the tissue. It should be noted that the integrals for gray and white matter are almost equal to the integral for plasma (Figure 4B). As can be seen from the operational equation, this phenomenon merely reflects the diminished contributions of the terms containing the exponential factors at 45 minutes after the pulse of [ $^{14}\text{C}$ ]DG; at infinite time all the integrals would be equal to the integral of the plasma curve. It may be recalled that the model assumes only a single compartment for free [ $^{14}\text{C}$ ]DG in each tissue. It can be shown that, at infinite time following a pulse, the integrals of the specific activities of all compartments, either in series or parallel, that derive their [ $^{14}\text{C}$ ]DG ultimately from the plasma compartment become equal to each other and to the integral of the plasma specific activity.\* It would then be immaterial if there were, indeed, more than one compartment, and 45 minutes is sufficiently close to infinity (i.e., at least 10 half-lives) to minimize possible errors due to that assumption.

### Experimental Protocol

The animals are prepared for the experiment by the insertion of polyethylene catheters in an artery and vein. Any convenient artery or vein can be used. In the rat the femoral or the tail arteries and veins have been found satisfactory. In the monkey and cat the femoral vessels are probably most convenient. The catheters are inserted under anesthesia, and anesthetic agents without long-lasting aftereffects should be used. Light halothane anesthesia, with or without supplementation with nitrous oxide, has been found to be quite satisfactory. At least two hours are allowed for recovery from the surgery and anesthesia before initiation of the experiment.

The design of the experimental procedure for the measurement of local cerebral glucose utilization was based on the theoretical considerations discussed above. At zero time a pulse of 125  $\mu\text{Ci}$  (no more than 2.5  $\mu\text{moles}$ ) of [ $^{14}\text{C}$ ]deoxyglucose per kg of body weight is

\*C. Patlak, unpublished.

administered to the animal via the venous catheter. Arterial sampling is initiated with the onset of the pulse, and timed 50- to 100- $\mu$ l samples of arterial blood are collected consecutively as rapidly as possible during the early period so as not to miss the peak of the arterial curve. Arterial sampling is continued at less frequent intervals later in the experimental period but at sufficient frequency to define fully the arterial curve. The arterial blood samples are immediately centrifuged to separate the plasma, which is stored on ice until assayed for [ $^{14}\text{C}$ ] DG by liquid scintillation counting and glucose concentrations by standard enzymatic methods. At approximately 45 minutes the animal is decapitated, and the brain is removed and frozen in Freon XII or isopentane maintained between  $-50^\circ$  and  $-75^\circ\text{C}$  with liquid nitrogen. When fully frozen, the brain is stored at  $-70^\circ\text{C}$  until sectioned and autoradiographed. The experimental period may be limited to 30 minutes. This is theoretically permissible and may sometimes be necessary for reasons of experimental expediency, but greater errors due to possible inaccuracies in the rate constants may result.

#### **Autoradiographic Measurement of Tissue $^{14}\text{C}$ Concentration**

The  $^{14}\text{C}$  concentrations in localized regions of the brain are measured by a modification of the quantitative autoradiographic technique previously described (Reivich et al., 1969). The frozen brain is coated with chilled embedding medium (Lipshaw Manufacturing Co., Detroit MI) and fixed to object-holders appropriate to the microtome to be used.

Brain sections, precisely 20  $\mu\text{m}$  in thickness, are prepared in a cryostat maintained at  $-21^\circ\text{C}$  to  $-22^\circ\text{C}$ . The brain sections are picked up on glass cover slips, dried on a hot plate at  $60^\circ\text{C}$  for at least 5 minutes, and placed sequentially in an X-ray cassette. A set of [ $^{14}\text{C}$ ]methylmethacrylate standards (Amersham Corp., Arlington Heights, IL), which include a blank and a series of progressively increasing  $^{14}\text{C}$  concentration, is also placed in the cassette. These standards must previously have been calibrated for their autoradiographic equivalence to the  $^{14}\text{C}$  concentrations in brain sections, 20  $\mu\text{m}$  in thickness, prepared as described above. The method of calibration has been described previously (Reivich et al., 1969).

Autoradiographs are prepared from these sections directly in the X-ray cassette with Kodak single-coated, blue-sensitive Medical X-ray Film, Type SB-5 (Eastman Kodak Co., Rochester, NY). The exposure time is generally 5 to 6 days with the doses used as described above, and the exposed films are developed according to the instructions supplied with the film. The SB-5 X-ray film is rapid but coarse-grained. For finer-grained autoradiographs and, therefore, better-defined

images with higher resolution, it is possible to use mammographic films, such as DuPont LoDose or Kodak MR-1 films, or fine-grain panchromatic film, such as Kodak Plus-X, but the exposure times are 2 to 3 times longer. The autoradiographs provide a pictorial representation of the relative  $^{14}\text{C}$  concentrations in the various cerebral structures and the plastic standards. A calibration curve of the relationship between optical density and tissue  $^{14}\text{C}$  concentrations for each film is obtained by densitometric measurements of the portions of the film representing the various standards. The local tissue concentrations are then determined from the calibration curve and the optical densities of the film in the regions representing the cerebral structures of interest. Local cerebral glucose utilization is calculated from the local tissue concentrations of  $^{14}\text{C}$  and the plasma [ $^{14}\text{C}$ ]DG and glucose concentrations according to the operational equation (Figure 2).

### Computerized Color-Coded Image-Processing

The autoradiographs provide pictorial representations of only the relative and not the actual rates of glucose utilization in all the structures of the nervous system. Furthermore, the resolution of differences in relative rates is limited by the ability of the human eye to recognize the differences in shades of gray. Manual densitometric analysis permits the computation of actual rates of glucose utilization with a fair degree of resolution, but it generates enormous tables of data that fail to convey the tremendous heterogeneity of metabolic rates, even within anatomic structures, or the full information contained within the autoradiographs. Gooch and coworkers (1980) have developed a computerized image-processing system to analyze and transform the autoradiographs into color-coded maps of the distribution of the actual rates of glucose utilization exactly where they are located throughout the central nervous system. The autoradiographs are scanned automatically by a computer-controlled scanning microdensitometer. The optical density of each spot in the autoradiograph, from 25 to 100  $\mu\text{m}$  as selected, is stored in a computer, converted to  $^{14}\text{C}$  concentration on the basis of the optical densities of the calibrated  $^{14}\text{C}$  plastic standards, and then converted to local rates of glucose utilization by solution of the operational equation of the method. Colors are assigned to narrow ranges of the rates of glucose utilization, and the autoradiographs are then displayed in a color TV monitor in color, along with a calibrated color scale for identifying the rate of glucose utilization in each spot of the autoradiograph from its color. These color maps add a third dimension, the rate of glucose utilization on a color scale, to the spatial dimensions already present on the autoradiographs.

## **RATES OF LOCAL CEREBRAL GLUCOSE UTILIZATION IN THE NORMAL CONSCIOUS STATE**

Thus far quantitative measurements of local cerebral glucose utilization have been reported only for the albino rat (Sokoloff et al., 1977) and monkey (Kennedy et al., 1978). These values are presented in Table 3. The rates of local cerebral glucose utilization in the normal conscious rat vary widely throughout the brain. The values in white structures tend to group together and are always considerably below those of gray structures. The average value in gray matter is approximately three times that of white matter, but the individual values vary from approximately 50 to 200  $\mu$ moles of glucose/100 g/min. The highest values are in the structures involved in auditory functions, with the inferior colliculus clearly the most metabolically active structure in the brain.

The rates of local cerebral glucose utilization in the conscious monkey exhibit similar heterogeneity, but they are generally one-third to one-half the values in corresponding structures of the rat brain (Table 3). The differences in rates in the rat and monkey brain are consistent with the different cellular packing densities in the brains of these two species.

## **EFFECTS OF GENERAL ANESTHESIA**

General anesthesia produced by thiopental reduces the rates of glucose utilization in all structures of the rat brain (Table 4) (Sokoloff et al., 1977). The effects are not uniform, however. The greatest reductions occur in the gray structures, particularly those of the primary sensory pathways. The effects in white matter, though definitely present, are relatively small compared to those of gray matter. These results are in agreement with those of previous studies in which anesthesia has been found to decrease the cerebral metabolic rate of the brain as a whole (Kety, 1950; Lassen, 1959; Sokoloff, 1976).

## **RELATION BETWEEN LOCAL FUNCTIONAL ACTIVITY AND ENERGY METABOLISM**

The results of a variety of applications of the method demonstrate a clear relationship between local cerebral functional activity and glucose consumption. The most striking demonstrations of the close coupling between function and energy metabolism are seen with experimentally induced local alterations in functional activity that are restricted to a few specific areas in the brain. The effects on local glucose consumption are then so pronounced that they are not only

**Table 3**  
 Representative Values for Local Cerebral Glucose Utilization in the Normal  
 Albino Rat and Monkey ( $\mu\text{moles}/100\text{g}/\text{min}$ )

Structure	Albino rat* (10)	Monkey† (7)
<b>Gray matter</b>		
Visual cortex	107 $\pm$ 6	59 $\pm$ 2
Auditory cortex	162 $\pm$ 5	79 $\pm$ 4
Parietal cortex	112 $\pm$ 5	47 $\pm$ 4
Sensory-motor cortex	120 $\pm$ 5	44 $\pm$ 3
Thalamus: lateral nucleus	116 $\pm$ 5	54 $\pm$ 2
Thalamus: ventral nucleus	109 $\pm$ 5	43 $\pm$ 2
Medial geniculate body	131 $\pm$ 5	65 $\pm$ 3
Lateral geniculate body	96 $\pm$ 2	39 $\pm$ 1
Hypothalamus	54 $\pm$ 2	25 $\pm$ 1
Mamillary body	121 $\pm$ 5	57 $\pm$ 3
Hippocampus	79 $\pm$ 3	39 $\pm$ 2
Amygdala	52 $\pm$ 2	25 $\pm$ 2
Caudate-putamen	110 $\pm$ 4	52 $\pm$ 3
Nucleus accumbens	82 $\pm$ 3	36 $\pm$ 2
Globus-pallidus	58 $\pm$ 2	26 $\pm$ 2
Substantia nigra	58 $\pm$ 3	29 $\pm$ 2
Vestibular nucleus	128 $\pm$ 5	66 $\pm$ 3
Cochlear nucleus	113 $\pm$ 7	51 $\pm$ 3
Superior olivary nucleus	133 $\pm$ 7	63 $\pm$ 4
Inferior colliculus	197 $\pm$ 10	103 $\pm$ 6
Superior colliculus	95 $\pm$ 5	55 $\pm$ 4
Pontine gray matter	62 $\pm$ 3	28 $\pm$ 1
Cerebellar cortex	57 $\pm$ 2	31 $\pm$ 2
Cerebellar nuclei	100 $\pm$ 4	45 $\pm$ 2
<b>White matter</b>		
Corpus callosum	40 $\pm$ 2	11 $\pm$ 1
Internal capsule	33 $\pm$ 2	13 $\pm$ 1
Cerebellar white matter	37 $\pm$ 2	12 $\pm$ 1

The values are the means  $\pm$  standard errors from measurements made in the number of animals indicated in parentheses.

\*From Sokoloff et al., 1977.

†From Kennedy et al., 1978.

**Table 4**

Effects of Thiopental Anesthesia on Local Cerebral Glucose Utilization in the Rat\*  
[Sokoloff et al., 1977]

Structure	Local cerebral glucose utilization ( $\mu$ moles/100g/min)		
	Control (6)†	Anesthetized (8)†	% Effect
<b>Gray matter</b>			
Visual cortex	111 $\pm$ 5	64 $\pm$ 3	- 42
Auditory cortex	157 $\pm$ 5	81 $\pm$ 3	- 48
Parietal cortex	107 $\pm$ 3	65 $\pm$ 2	- 39
Sensory-motor cortex	118 $\pm$ 3	67 $\pm$ 2	- 43
Lateral geniculate body	92 $\pm$ 2	53 $\pm$ 3	- 42
Medial geniculate body	126 $\pm$ 6	63 $\pm$ 3	- 50
Thalamus: lateral nucleus	108 $\pm$ 3	58 $\pm$ 2	- 46
Thalamus: ventral nucleus	98 $\pm$ 3	55 $\pm$ 1	- 44
Hypothalamus	63 $\pm$ 3	43 $\pm$ 2	- 32
Caudate-putamen	111 $\pm$ 4	72 $\pm$ 3	- 35
Hippocampus: Ammon's horn	79 $\pm$ 1	56 $\pm$ 1	- 29
Amygdala	56 $\pm$ 4	41 $\pm$ 2	- 27
Cochlear nucleus	124 $\pm$ 7	79 $\pm$ 5	- 36
Lateral lemniscus	114 $\pm$ 7	75 $\pm$ 4	- 34
Inferior colliculus	198 $\pm$ 7	131 $\pm$ 8	- 34
Superior olivary nucleus	141 $\pm$ 5	104 $\pm$ 7	- 26
Superior colliculus	99 $\pm$ 3	59 $\pm$ 3	- 40
Vestibular nucleus	133 $\pm$ 4	81 $\pm$ 4	- 39
Pontine gray matter	69 $\pm$ 3	46 $\pm$ 3	- 33
Cerebellar cortex	66 $\pm$ 2	44 $\pm$ 2	- 33
Cerebellar nucleus	106 $\pm$ 4	75 $\pm$ 4	- 29
<b>White matter</b>			
Corpus callosum	42 $\pm$ 2	30 $\pm$ 2	- 29
Genu of corpus callosum	35 $\pm$ 5	30 $\pm$ 2	- 14
Internal capsule	35 $\pm$ 2	20 $\pm$ 2	- 17
Cerebellar white matter	38 $\pm$ 2	29 $\pm$ 2	- 24

\*Determined at 30 min following pulse of [ $^{14}$ C] deoxyglucose.

†The values are the means  $\pm$  standard errors obtained in the number of animals indicated in parentheses. All the differences are statistically significant at the  $p < 0.05$  level.

observed in the quantitative results but can be visualized directly on the autoradiographs, which are really pictorial representations of the relative rates of glucose utilization in the various structural components of the brain.

### **Effects of Increased Functional Activity**

#### *Effects of Sciatic Nerve Stimulation*

Electrical stimulation of one sciatic nerve in the rat under barbiturate anesthesia causes pronounced increases in glucose consumption (i.e., increased optical density in the autoradiographs) in the ipsilateral dorsal horn of the lumbar spinal cord (Kennedy et al., 1975).

#### *Effects of Olfactory Stimulation*

The [<sup>14</sup>C]deoxyglucose method has been used to map the olfactory system of the rat (Sharp et al., 1975). Olfactory stimulation with amyl acetate has been found to produce increased labeling in localized regions of the olfactory bulb. Preliminary results obtained with other odors, such as camphor and cheese, suggest different spatial patterns of increased metabolic activity with different odors.

#### *Effects of Experimental Focal Seizures*

The local injection of penicillin into the hand-face area of the motor cortex of the Rhesus monkey has been shown to induce electrical discharges in the adjacent cortex and to result in recurrent focal seizures involving the face, arm, and hand on the contralateral side (Caveness, 1969). Such seizure activity causes selective increases in glucose consumption in areas of motor cortex adjacent to the penicillin locus and in small discrete regions of the putamen, globus pallidus, caudate nucleus, thalamus, and substantia nigra of the same side (Figure 5) (Kennedy et al., 1975). Similar studies in the rat have led to comparable results and have provided evidence on the basis of an evoked metabolic response of a "mirror" focus in the motor cortex contralateral to the penicillin-induced epileptogenic focus (Collins et al., 1976).

### **Effects of Decreased Functional Activity**

Decrements in functional activity result in reduced rates of glucose utilization. These effects are particularly striking in the auditory and visual systems of the rat and the visual system of the monkey.

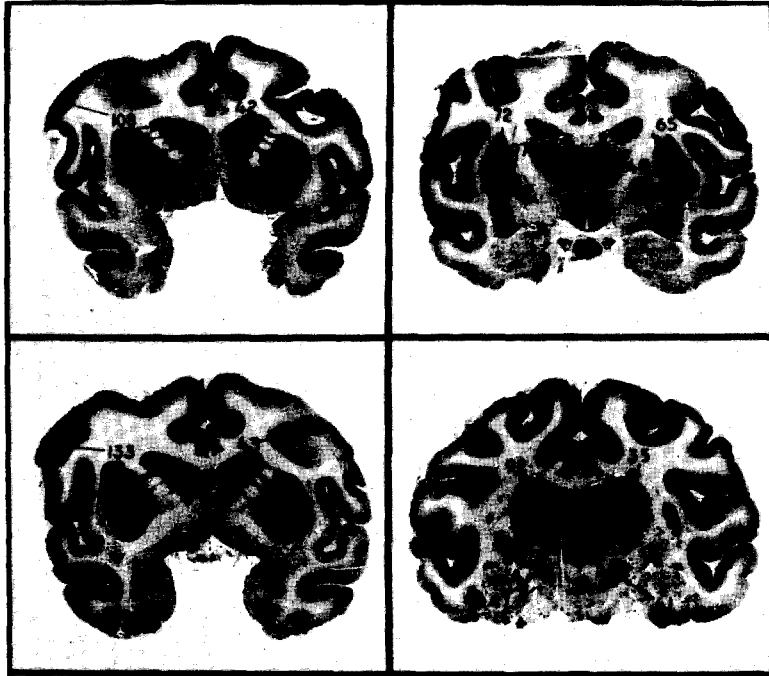


**Figure 5.**

Effects of focal seizures produced by local application of penicillin to motor cortex on local cerebral glucose utilization in the Rhesus monkey. The penicillin was applied to the hand and face area of the left motor cortex. The left side of the brain is on the left in each of the autoradiographs in the figure. The numbers are the rates of local cerebral glucose utilization in  $\mu\text{mol}/100\text{ g tissue}/\text{min}$ . Note the following: *upper left*, motor cortex in region of penicillin application and corresponding region of contralateral motor cortex; *lower left*, ipsilateral and contralateral motor cortical regions remote from area of penicillin applications; *upper right*, ipsilateral and contralateral putamen and globus pallidus; *lower right*, ipsilateral and contralateral thalamic nuclei and substantia nigra. [Sokoloff, 1977]

### *Effects of Auditory Deprivation*

In the albino rat some of the highest rates of local cerebral glucose utilization are found in components of the auditory system; i.e., auditory cortex, medial geniculate ganglion, inferior colliculus, lateral lemniscus, superior olive, and cochlear nucleus (Table 3). Bilateral auditory deprivation by occlusion of both external auditory canals with wax markedly depresses the metabolic activity in all of these areas (Sokoloff, 1977). The reductions are symmetrical bilaterally and range from 35 to 60%. Unilateral auditory deprivation also depresses the glucose consumption of these structures, but to a lesser degree, and some of the structures are asymmetrically affected. For example, the metabolic activity of the ipsilateral cochlear nucleus equals 75% of the activity of the contralateral nucleus. The lateral lemniscus, superior olive, and medial geniculate ganglion are slightly lower on the contralateral side, while the contralateral inferior colliculus is markedly lower in metabolic activity than the ipsilateral structure. These results demonstrate that there is some degree of lateralization and crossing of auditory pathways in the rat.

### *Visual Deprivation in the Rat*

In the rat, the visual system is 80 to 85% crossed at the optic chiasma (Lashley, 1934; Montero and Guillery, 1968), and unilateral enucleation removes most of the visual input to the central visual structures of the contralateral side. In the conscious rat studied 2 to 24 hours after unilateral enucleation, there are marked decrements in glucose utilization in the contralateral superior colliculus, lateral geniculate ganglion, and visual cortex as compared to the ipsilateral side (Kennedy et al., 1975).

### *Visual Deprivation in the Monkey*

In animals with binocular visual systems, such as the Rhesus monkey, there is only approximately 50% crossing of the visual pathways, and the structures of the visual system on each side of the brain receive equal inputs from both retinas. Although each retina projects more or less equally to both hemispheres, their projections remain segregated and terminate in six well-defined laminae in the lateral geniculate ganglia, three each for the ipsilateral and contralateral eyes (Hubel and Wiesel, 1968, 1972; Wiesel et al., 1974; Rakic, 1976). This segregation is preserved in the optic radiations that project the monocular representations of the two eyes for any segment of the visual field to adjacent regions of Layer IV of the striate cortex (Hubel and Wiesel, 1968, 1972). The cells responding to the input of each monocular terminal zone are distributed transversely through the thickness of the

striate cortex, resulting in a mosaic of columns, 0.3 to .5 mm in width, alternately representing the monocular inputs of the two eyes. The nature and distribution of these ocular dominance columns have previously been characterized by electrophysiological techniques (Hubel and Wiesel, 1968), Nauta degeneration methods (Hubel and Wiesel, 1972), and by autoradiographic visualization of axonal and transneuronal transport of [ $^3\text{H}$ ]proline- and [ $^3\text{H}$ ]fucose-labeled protein and/or glycoprotein (Wiesel et al., 1974; Rakic, 1976). Bilateral or unilateral visual deprivation, either by enucleation or by the insertion of opaque plastic discs, produces consistent changes in the pattern of distribution of the rates of glucose consumption, all clearly visible in the autoradiographs, that coincide closely with the changes in functional activity expected from known physiological and anatomical properties of the binocular visual system (Kennedy et al., 1976).

In animals with intact binocular vision, no bilateral asymmetry is seen in the autoradiographs of the structures of the visual system (Figures 6A and 7A). The lateral geniculate ganglia and oculomotor nuclei appear to be of fairly uniform density and essentially the same on both sides (Figure 6A). The visual cortex is also the same on both sides (Figure 7A), but throughout all of Area 17 there is heterogeneous density distributed in a characteristic laminar pattern. These observations indicate that, in animals with binocular visual input, the rates of glucose consumption in the visual pathways are essentially equal on both sides of the brain and relatively uniform in the oculomotor nuclei and lateral geniculate ganglia but markedly different in the various layers of the striate cortex.

Autoradiographs from animals with both eyes occluded exhibit generally decreased labeling of all components of the visual system, but the bilateral symmetry is fully retained (Figures 6B and 7B), and the density within each lateral geniculate body is for the most part fairly uniform (Figure 6B). In the striate cortex, however, the marked differences in the densities of the various layers seen in the animals with intact bilateral vision (Figure 7A) are virtually absent so that, except for a faint delineation of a band within Layer IV, the concentration of the label is essentially homogeneous throughout the striate cortex (Figure 7B).

Autoradiographs from monkeys with only monocular input, because of unilateral visual occlusion, exhibit markedly different patterns from those described above. Both lateral geniculate bodies exhibit exactly inverse patterns of alternating dark and light bands, corresponding to the known laminae representing the regions receiving the different inputs from the retinas of the intact and occluded eyes (Figure 6C). Bilateral asymmetry is also seen in the oculomotor nuclear complex;



5.0mm

**Figure 6.**

Autoradiography of coronal brain sections of monkey at the level of the lateral geniculate bodies. Large arrows point to the lateral geniculate bodies; small arrows point to oculomotor nuclear complex. A. Animal with intact binocular vision. Note the bilateral symmetry and relative homogeneity of the lateral geniculate bodies and oculomotor nuclei. B. Animal with bilateral visual occlusion. Note the reduced relative densities, the relative homogeneity, and the bilateral symmetry of the lateral geniculate bodies and oculomotor nuclei. C. Animal with right eye occluded. The left side of the brain is on the left side of the photograph. Note the laminae and the inverse order of the dark and light bands in the two lateral geniculate bodies. Note also the lesser density of the oculomotor nuclear complex on the side contralateral to the occluded eye. [Kennedy et al., 1976]

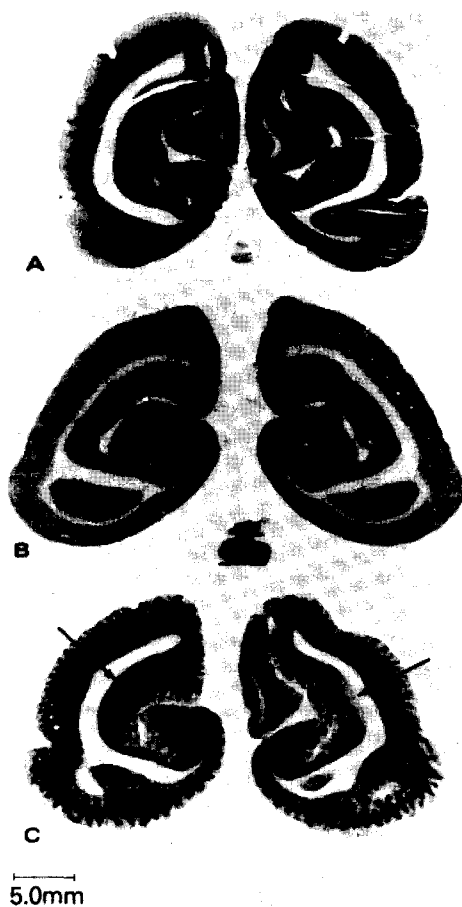


**Figure 7.**

Autoradiographs of coronal brain sections from Rhesus monkeys at the level of the striate cortex. A. Animal with normal binocular vision. Note the laminar distribution of the density; the dark band corresponds to Layer IV. B. Animal with bilateral visual deprivation. Note the almost uniform and reduced relative density, especially the virtual disappearance of the dark band corresponding to Layer IV. C. Animal with right eye occluded. The half-brain on the left side of the photograph represents the left hemisphere contralateral to the occluded eye. Note the alternate dark and light striations, each approximately 0.3 to 0.4 mm in width, that represent the ocular dominance columns. These columns are most apparent in the dark band corresponding to Layer IV but extend through the entire thickness of the cortex. The arrows point to regions of bilateral asymmetry where the ocular dominance columns are absent. These are presumably areas with normally only monocular input. The one on the left, contralateral to occluded eye, has a continuous dark lamina corresponding to Layer IV, which is completely absent on the side ipsilateral to the occluded eye. These regions are believed to be the loci of the cortical representations of the blind spots. [Kennedy et al., 1976]

a lower density is apparent in the nuclear complex contralateral to the occluded eye (Figure 6C). In the striate cortex, the pattern of distribution of the [ $^{14}\text{C}$ ]DG-6-P appears to be a composite of the patterns seen in the animals with intact and bilaterally occluded visual input. The pattern found in the former regularly alternates with that of the latter in columns oriented perpendicularly to the cortical surface (Figure 7C). The dimensions, arrangement, and distribution of these columns are identical to those of the ocular dominance columns described by Hubel and Wiesel (Hubel and Wiesel, 1968, 1972; Wiesel et al., 1974). These columns reflect the interdigitation of the representations of the two retinas in the visual cortex. Each element in the visual fields is represented by a pair of contiguous bands in the visual cortex, one for each of the two retinas or their portions that correspond to a given point in the visual fields. With symmetrical visual input bilaterally, the columns representing the two eyes are equally active and, therefore, not visualized in the autoradiographs (Figure 7A). When one eye is blocked, however, only those columns representing the blocked eye become metabolically less active, and the autoradiographs then display the alternate bands of normal and depressed activities corresponding to the regions of visual cortical representation of the two eyes (Figure 7C).

There can be seen in the autoradiographs from the animals with unilateral visual deprivation a pair of regions in the folded calcarine cortex that exhibit bilateral asymmetry (Figure 7C). The ocular dominance columns are absent on both sides, but on the side contralateral to the occluded eye this region has the appearance of visual cortex from an animal with normal bilateral vision, and on the ipsilateral side this region looks like cortex from an animal with both eyes occluded (Figure 7). These regions are the loci of the cortical representation of the blind spots of the visual fields and normally have only monocular input (Kennedy et al., 1975, 1976). The area of the optic disc in the nasal half of each retina cannot transmit to this region of the contralateral striate cortex which, therefore, receives its sole input from an area in the temporal half of the ipsilateral retina. Occlusion of one eye deprives this region of the ipsilateral striate cortex of all input, while the corresponding region of the contralateral striate cortex retains uninterrupted input from the intact eye. The metabolic reflection of this ipsilateral monocular input is seen in the autoradiograph in Figure 7C.

The results of these studies with the [ $^{14}\text{C}$ ]deoxyglucose method in the binocular visual system of the monkey represent the most dra-

matic demonstration of the close relationship between physiological changes in functional activity and the rate of energy metabolism in specific components of the central nervous system.

### **MECHANISM OF COUPLING OF LOCAL FUNCTIONAL ACTIVITY AND ENERGY METABOLISM**

In tissues like heart muscle, skeletal muscle, and kidney, which do readily recognizable physical work, there is a clear quantitative relationship between the work performed and the rate of energy metabolism. Presumably, at least part of the energy derived from metabolism is equivalent to the energy expenditure associated with the physical work and serves to resynthesize high-energy phosphate bonds consumed in the process. It is less clear what physical work is performed by nervous tissue. The finding of a close coupling between local functional activity and glucose utilization suggests, however, that neural functional activity is associated with some energy-consuming physical and/or chemical processes.

Electrical activity appears to be the physical process most intimately involved with functional activity in nervous tissue. Action potentials are generated by the movement of ions, mainly  $\text{Na}^+$  and  $\text{K}^+$ , across cell membranes down ionic gradients, and energy must be consumed to restore the ionic gradients to their resting levels. Increased electrical activity, i.e., increased frequency of action potentials, might be expected to lead to greater ionic fluxes and require, therefore, more energy to restore the ionic gradients. Indeed, Yarowsky and coworkers (1979) have recently found in the superior cervical ganglion *in vivo* a direct linear relationship between the frequency of the electrical spike input and the rate of glucose utilization (see below). The energy required to transport the ions back across the cell membrane to restore the ionic gradients is presumably derived from the splitting of ATP by  $\text{Na}^+$ ,  $\text{K}^+$ -ATPase (Albers, 1967; Caldwell, 1968). Once ATP is split, there are adequate biochemical mechanisms to explain the increased glucose utilization and energy metabolism. It has been estimated that more than 40% of the energy consumption of the brain is used for the maintenance and restoration of ionic gradients and membrane potentials (Whittam, 1962).

This hypothesis implies that the  $\text{Na}^+$ ,  $\text{K}^+$ -ATPase is a key link in the coupling of glucose utilization to functional activity. To test this hypothesis, Mata and coworkers, (1980) have used the  $[^{14}\text{C}]$  deoxyglucose technique *in vitro* with electrically stimulated preparations of

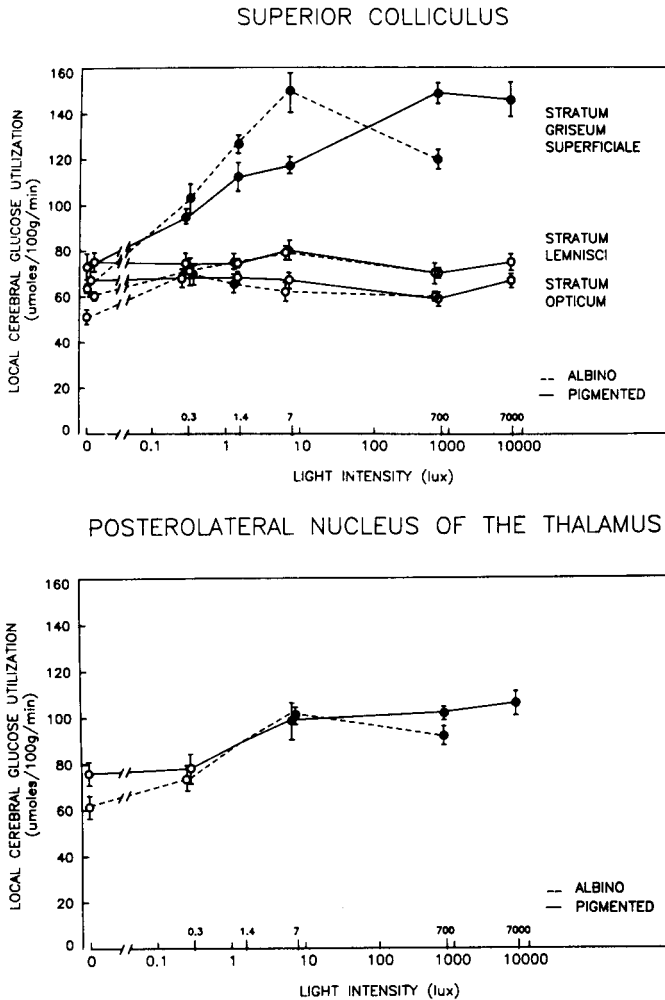
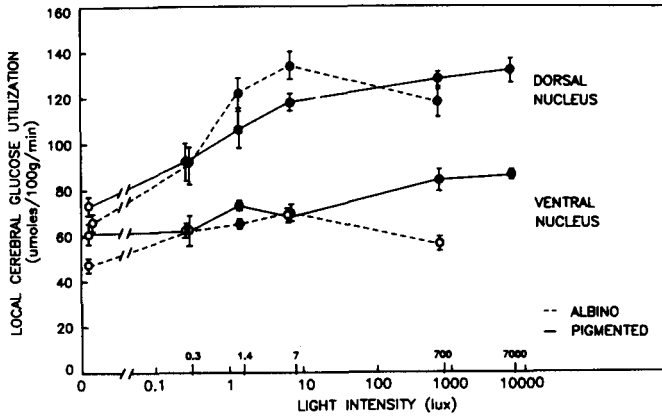


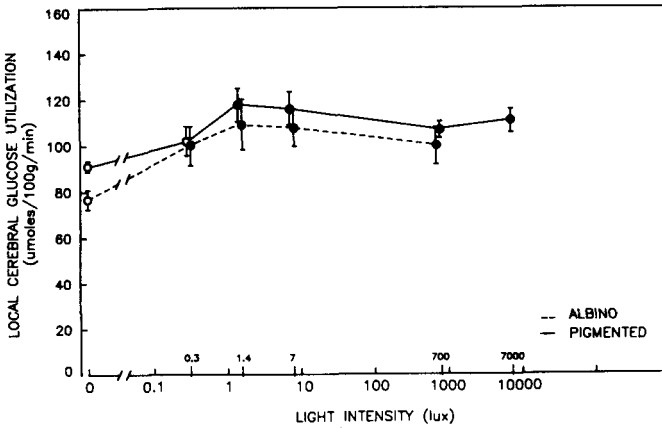
**Figure 8.** Effects of intensity of retinal illumination with randomly spaced light flashes on local cerebral glucose utilization in components of the visual system of the albino and Norway brown rat.

rat posterior pituitary. Electrical stimulation led to increased glucose utilization that was blocked by ouabain, an inhibitor of the  $\text{Na}^+$ ,  $\text{K}^+$ -ATPase but not of the spike activity or the release of vasopressin by the gland. It is noteworthy that veratridine, an alkaloid that opens

LATERAL GENICULATE NUCLEUS



VISUAL CORTEX



Note that the local glucose utilization is proportional to the logarithm of the intensity of illumination, at least at lower levels of intensity, in the primary projection areas of the retina. [Miyaoaka et al., 1979a]

Na<sup>+</sup> channels, depolarizes the cell membranes, and, therefore, activates Na<sup>+</sup>, K<sup>+</sup>-ATPase activity, also stimulated glucose utilization in the posterior pituitary, and this effect was also blocked by ouabain or tetrodotoxin. These results strongly support the hypothesis that

## COLOR PLATES

### Figure 9.

Metabolic activation of "whisker barrel" in right sensory cortex of rat by stroking of single vibrissa on left side of face. The upper left panel includes the entire section of the rat brain at the level of the "whisker barrel". Successive panels illustrate the results of rescanning at higher resolution and/or zooming. The lower right panel includes a scan at highest resolution; each pixel is equivalent to 25  $\mu\text{m}$ . The experiment was carried out by Hand and coworkers (1978), and the color-coded image-processing was done by the method of Gooch and coworkers (1980). [Hand, 1981]

### Figure 10A.

Metabolic activation of the motor and sensory systems of conscious monkey conditioned to move its left hand and arm 10 to 20 times per min throughout the experimental period. Sections through brain and cervical spinal cord. *Upper right*: note increased metabolic activity in the contralateral motor and sensory cortex and the thalamus. *Lower right*: note the increased glucose utilization in the contralateral motor and sensory cortex and globus pallidus. *Lower left*: note the increased metabolism in the ipsilateral cerebellum and cuneate nucleus. *Upper left*: note the increased metabolic rate in the ventral and dorsal horns of the cervical spinal cord on the side ipsilateral to the arm movement. [Kennedy et al., 1980]

### Figure 10B.

Metabolic activation of the motor and sensory systems of conscious monkey conditioned to move its left hand and arm 10 to 20 times/min throughout the experimental period. Sections through spinal cord between first cervical and first thoracic segments. Note increased metabolic activities in left ventral and dorsal horns of segments of cervical cord involved in movement of left hand and arm. [Kennedy et al., 1980]

### Figure 13.

Retina-dependent activation of metabolic activity by apomorphine in superficial layer of superior colliculus of the rat. *Left*, control rat, with right eye enucleated, administered saline intravenously. *Right*, experimental rat, with right eye unenucleated, administered 1.5 mg/kg of apomorphine intravenously. Note the bilateral metabolic activation of the deep layers of the superior colliculus but metabolic activation in the superficial layer only in the ipsilateral superior colliculus and no response in the superficial layer contralateral to the enucleated eye. [McCulloch et al., 1980b]

### Figure 15.

Influence of visual input on glucose utilization of human cerebral cortex. *Left column*: three horizontal sections of brain of normal conscious man studied with [ $^{18}\text{F}$ ]fluorodeoxyglucose technique while eyes were open. *Right column*: same three sections studied with eyes closed. Note the decreased glucose utilization in the occipital cortex and the increased metabolic activity in the frontal cortex when the eyes are closed. [Phelps et al., 1980]

### Figure 16.

Changes in local cerebral utilization in a human patient with partial complex epilepsy during seizures. The three images were obtained from the same section of brain studied three times with the [ $^{18}\text{F}$ ]fluorodeoxyglucose technique. *Left*: patient in interictal state. Note the area with the low rate of glucose utilization in the left temporal cortex compared to the comparable area on the right. *Middle*: patient suffering from severe seizure. Note the marked increase in glucose utilization in the left temporal cortex and the generalized decrease in metabolic activity throughout the remainder of the cerebral cortex. *Right*: patient suffering from more moderate seizure. Note the increased glucose utilization in the left temporal cortex and the decreased metabolic activity in the remainder of the cerebral cortex of the left side only. [Kuhl et al., in press]

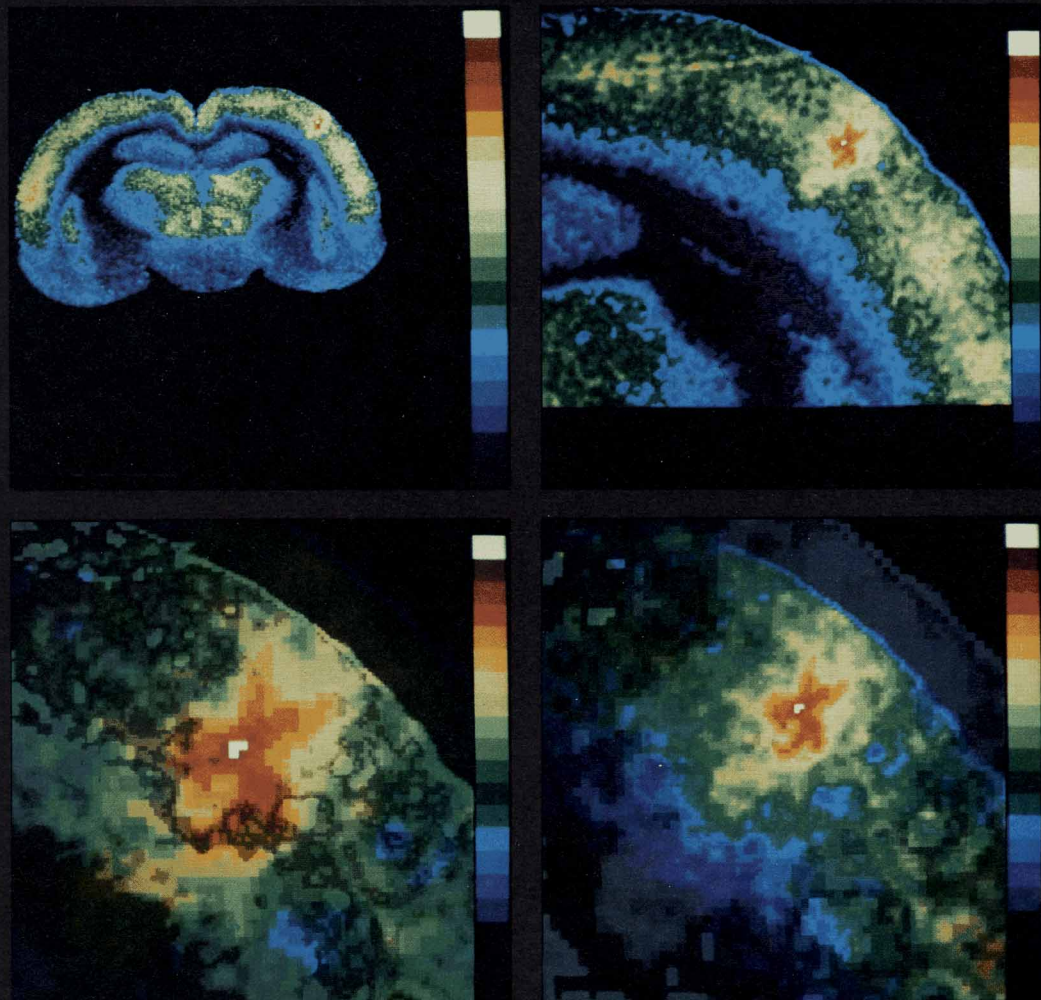


Figure 9

LOCAL CEREBRAL GLUCOSE UTILIZATION

MONKEY USING LEFT ARM

UMOLES  
/100G  
/MIN

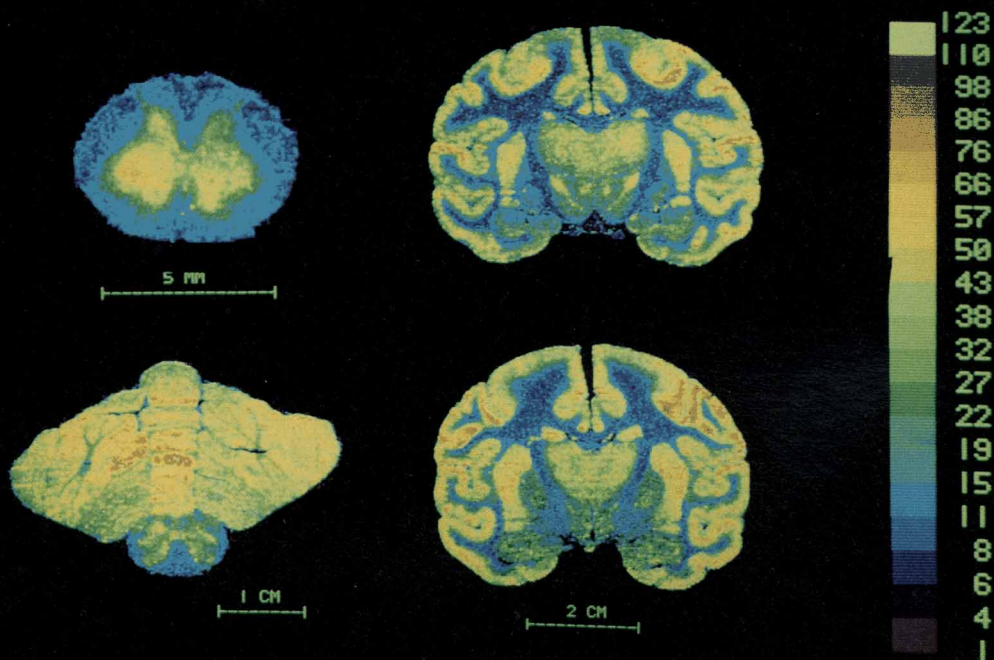


Figure 10A

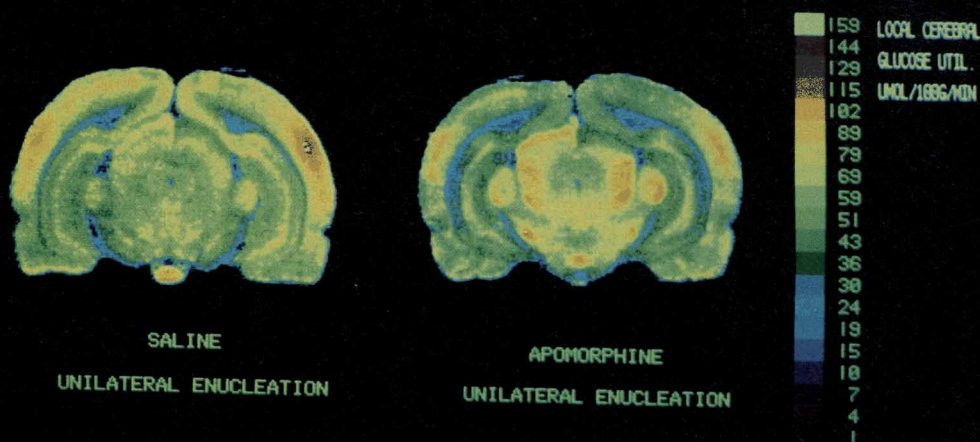


Figure 13

GLUCOSE UTILIZATION IN SPINAL CORD  
OF MONKEY USING ONE ARM

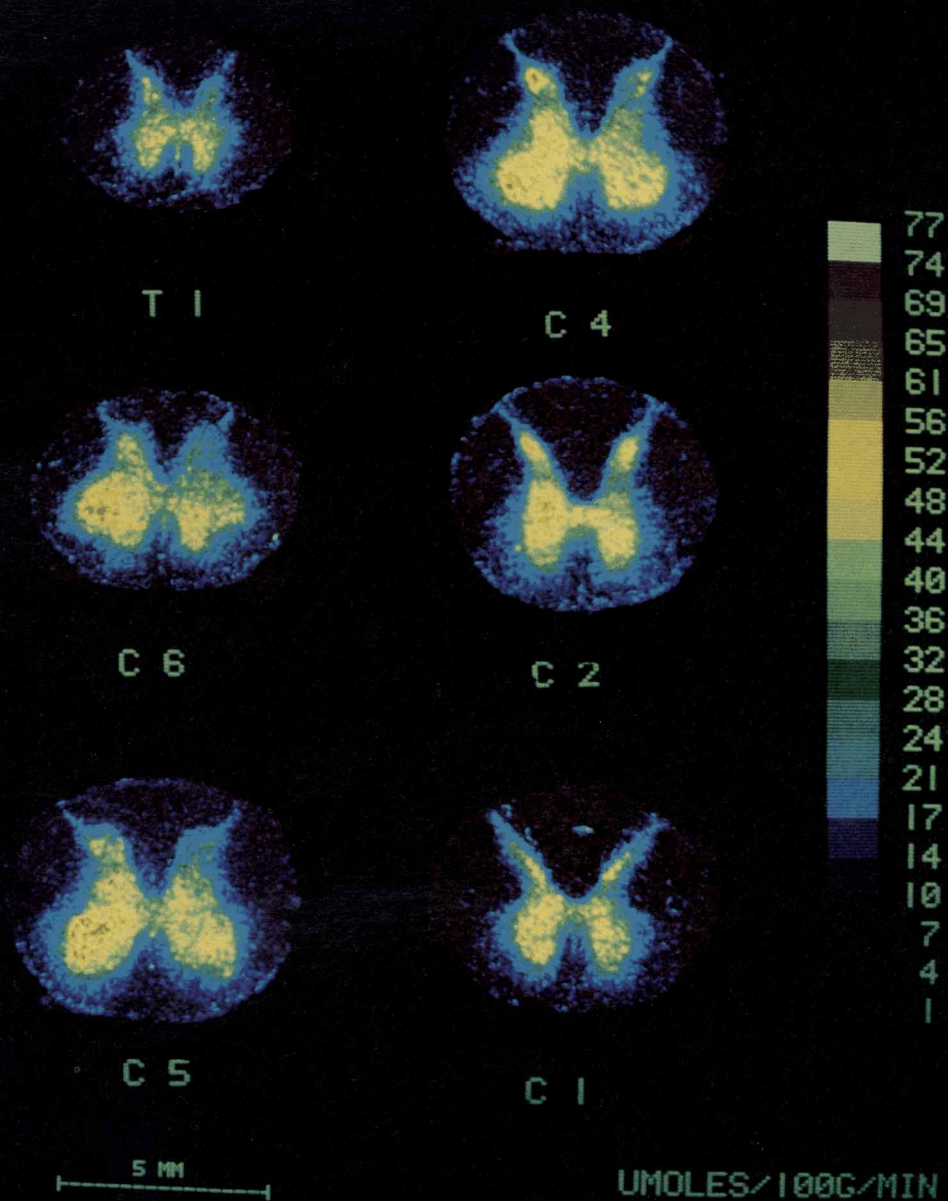
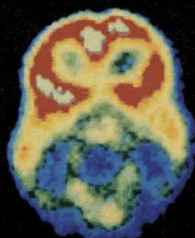
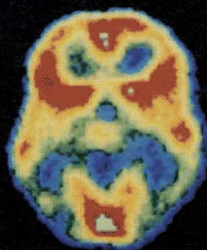
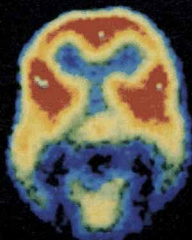
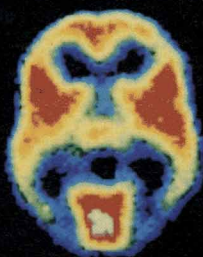
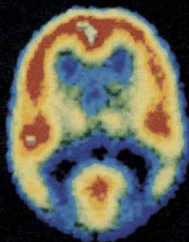


Figure 10B

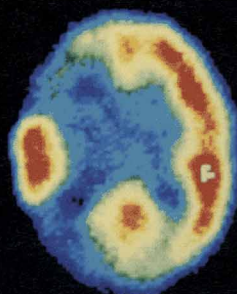
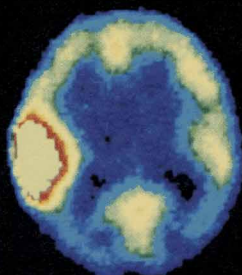
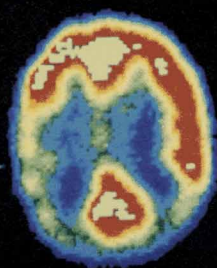
EYES OPEN

EYES CLOSED



ECAT IMAGES BY PHELPS AND KUHL / COLOR-CODING BY LCM-NIMH

Figure 15



INTERICTAL

ICTAL I

ICTAL II

Figure 16

energy metabolism is coupled to functional activity through the activity of the  $\text{Na}^+$ ,  $\text{K}^+$ -ATPase.

The posterior pituitary is highly enriched with axon terminals that account for more than 42% of the gland's total volume (Nordmann, 1977). The gland contains, therefore, an extraordinarily high content of elements with large areas of membrane surface relative to their volumes. Such structures are likely to suffer relatively large changes in ionic concentration gradients for a given amount of electrical spike activity. The increased glucose utilization observed by Mata and colleagues (1980) in the electrically stimulated posterior pituitary in vitro probably reflected mainly the metabolic activity of the axonal terminals. Schwartz and coworkers (1979) have studied the entire hypothalamo-hypophysial pathway in vivo by means of the [ $^{14}\text{C}$ ]-deoxyglucose method. Stimulation of this pathway physiologically by salt-loading also led to markedly increased glucose utilization in the posterior pituitary, but surprisingly, there were no detectable effects in the supraoptic and paraventricular nuclei, the loci of the cell bodies with projections to the posterior pituitary. Obviously the pathway had been activated by the osmotic stimulation. The discrepancy in the effects in the cell bodies and in the regions of termination of their projections may well reflect the greater sensitivity of axonal terminals and/or synaptic elements than that of perikarya to metabolic activation. Indeed, the results of the studies on the binocular system of the monkey described above also lend support to this possibility. In the animals with both eyes open, Layer IVB, the layer with predominantly neuropil and axodendritic connections, is clearly the most metabolically active portion of the striate cortex (Kennedy et al., 1976) (Figure 7A). It is precisely this region that shows the greatest reduction in glucose utilization when both eyes are patched; the other layers also exhibit some reductions in metabolism but much less so, and Layer IVB can then hardly be distinguished from the other layers in the autoradiographs (Figure 7B). It seems likely, then, that the changes in local cerebral glucose utilization in response to altered functional activity revealed by the [ $^{14}\text{C}$ ]deoxyglucose method represent mainly alterations in the metabolic activity of synaptic terminals triggered by changes in  $\text{Na}^+$ ,  $\text{K}^+$ -ATPase activity.

## APPLICATIONS OF THE DEOXYGLUCOSE METHOD

The results of studies like those described above on the effects of experimentally induced focal alterations of functional activity on local

glucose utilization have demonstrated a close coupling between local functional activity and energy metabolism in the central nervous system. The effects are often so pronounced that they can be visualized directly on the autoradiographs, which provide pictorial representations of the relative rates of glucose utilization throughout the brain. This technique of autoradiographic visualization of evoked metabolic responses offers a powerful tool to map functional neural pathways simultaneously in all anatomical components of the central nervous system, and extensive use has been made of it for this purpose (Plum et al., 1976). The results have clearly demonstrated the effectiveness of metabolic responses, either positive or negative, in identifying regions of the central nervous system involved in specific functions.

The method has been used most extensively in qualitative studies in which regions of altered functional activity are identified by the change in their visual appearance relative to other regions in the autoradiographs. Such qualitative studies are useful only when the effects are lateralized to one side or when only a few discrete regions are affected; other regions serve as the controls. Quantitative comparisons cannot, however, be made for equivalent regions between two or more animals. To make quantitative comparisons between animals, the fully quantitative method must be used, which takes into account the various factors, particularly the plasma glucose level, that influence the magnitude of labeling of the tissues. The method must be used quantitatively when the experimental procedure produces systemic effects and alters metabolism in many regions of the brain.

A comprehensive review of the many qualitative and quantitative applications of the method is beyond the scope of this report. Only some of the many neurophysiological, neuroanatomical, pharmacological, and pathophysiological applications of the method will be briefly noted merely to illustrate the broad extent of its potential usefulness.

### **Neurophysiological and Neuroanatomical Applications**

Many of the physiological applications of the [ $^{14}\text{C}$ ]deoxyglucose method were in studies designed to test the method and to examine the relationship between local cerebral functional and metabolic activities. These applications have been described above. The most dramatic results have been obtained in the visual systems of the monkey and the rat. The method has, for example, been used to define the nature, conformation, and distribution of the ocular dominance columns in the striate cortex of the monkey (Figure 7C) (Kennedy et al., 1976). It has been used by Hubel and coworkers (1978) to do the same for the orientation columns in the striate cortex of the mon-

key. A by-product of the studies of the ocular dominance columns was the identification of the loci of the visual cortical representation of the blind spots of the visual fields (Figure 7C) (Kennedy et al., 1976). Studies are currently in progress to map the pathways of higher visual functions beyond the striate cortex; the results thus far demonstrate extensive areas of involvement of the inferior temporal cortex in visual processing (Jarvis et al., 1978). Des Rosiers and colleagues (1978) have used the method to demonstrate functional plasticity in the striate cortex of the infant monkey. The ocular dominance columns are already present on the first day of life, but if one eye is kept patched for three months, the columns representing the open eye broaden and completely take over the adjacent regions of cortex containing the columns for the eye that had been patched. Inasmuch as there is no longer any cortical representation for the patched eye, the animal becomes functionally blind in one eye. This phenomenon is almost certainly the basis for the cortical blindness or amblyopia that often occurs in children with uncorrected strabismus.

There have also been extensive studies of the visual system of the rat. This species has little if any binocular vision and, therefore, lacks the ocular dominance columns. Batipps and collaborators (1981) have compared the rates of local cerebral glucose utilization in albino and Norway brown rats. The rates were essentially the same throughout the brain except in the components of the primary visual system. The metabolic rates in the superior colliculus, lateral geniculate, and visual cortex of the albino rat were significantly lower than those in the pigmented rat. Miyaoka and coworkers (1979a) have studied the influence of the intensity of retinal stimulation with randomly spaced light flashes on the metabolic rates in the visual systems of the two strains. In dark-adapted animals there is relatively little difference between the two strains. With increasing intensity of light, the rates of glucose utilization first increase in the primary projection areas of the retina, e.g., superficial layer of the superior colliculus and lateral geniculate body, and the slopes of the increase are steeper in the albino rat (Figure 8). At 7 lux, however, the metabolic rates peak in the albino rat and then decrease with increasing light intensity. In contrast, the metabolic rates in the pigmented rat rise until they reach a plateau at about 700 lux, approximately the ambient light intensity in the laboratory. At this level, the metabolic rates in the visual structures of the albino rat are considerably below those of the pigmented rat. These results are consistent with the greater intensity of light reaching the visual cells of the retina in the albino rats because of lack of pigment and the subsequent damage to the rods at higher light intensities. It is of considerable interest that the rates of glucose

utilization in these visual structures obey the Weber-Fechner Law, i.e., the metabolic rate is directly proportional to the logarithm of the intensity of stimulation (Miyaoaka et al., 1979a). Inasmuch as this law was first developed from behavioral manifestations, these results simply imply that there is a quantitative relationship between behavioral and metabolic responses.

Although less extensive, there have also been applications of the method to other sensory systems. Studies of the olfactory system (Sharp et al., 1975) have been discussed above. In addition to the experiments in the auditory system described above, there have been studies of tonotopic representation in the auditory system. Webster and coworkers (1978) have obtained clear evidence of selective regions of metabolic activation in the cochlear nucleus, superior olivary complex, nuclei of the lateral lemnisci, and the inferior colliculus in cats in response to different frequencies of auditory stimulation. Similar results have been obtained by Silverman and coworkers (1977) in the rat and guinea pig. Studies of the sensory cortex have demonstrated metabolic activation of the "whisker barrels" by stimulation of the whiskers in the rat (Durham and Woolsey, 1977; Hand et al., 1978). Each whisker is represented in a discrete region of the sensory cortex; their precise location and extent have been elegantly mapped by Hand and coworkers (1978) and Hand (1980) by means of the [ $^{14}\text{C}$ ]deoxyglucose method (Figure 9: see color insert).

Thus far, there has been relatively little application of the method to the physiology of motor functions. Kennedy and collaborators (1980) have studied monkeys that were conditioned to perform a task with one hand in response to visual cues; in the monkeys that were performing, they observed metabolic activation throughout the appropriate areas of the motor as well as sensory systems from the cortex to the spinal cord (Figure 10: see color insert).

An interesting physiological application of the [ $^{14}\text{C}$ ]deoxyglucose method has been to the study of circadian rhythms in the central nervous system. Schwartz and his coworkers (1977, 1980) found that the suprachiasmatic nucleus in the rat exhibits circadian rhythmicity in metabolic activity, high during the day and low during the night (Figure 11). None of the other structures that they examined in the brain showed rhythmic activity. The normally low activity present in the nucleus in the dark could be markedly increased by light, but darkness did not reduce the glucose utilization during the day. The rhythm is entrained to light; reversal of the light-dark cycle leads not only to reversal of the rhythm in running activity but also in the cycle of metabolic activity in the suprachiasmatic nucleus. These studies lend support to the idea that the suprachiasmatic nucleus has

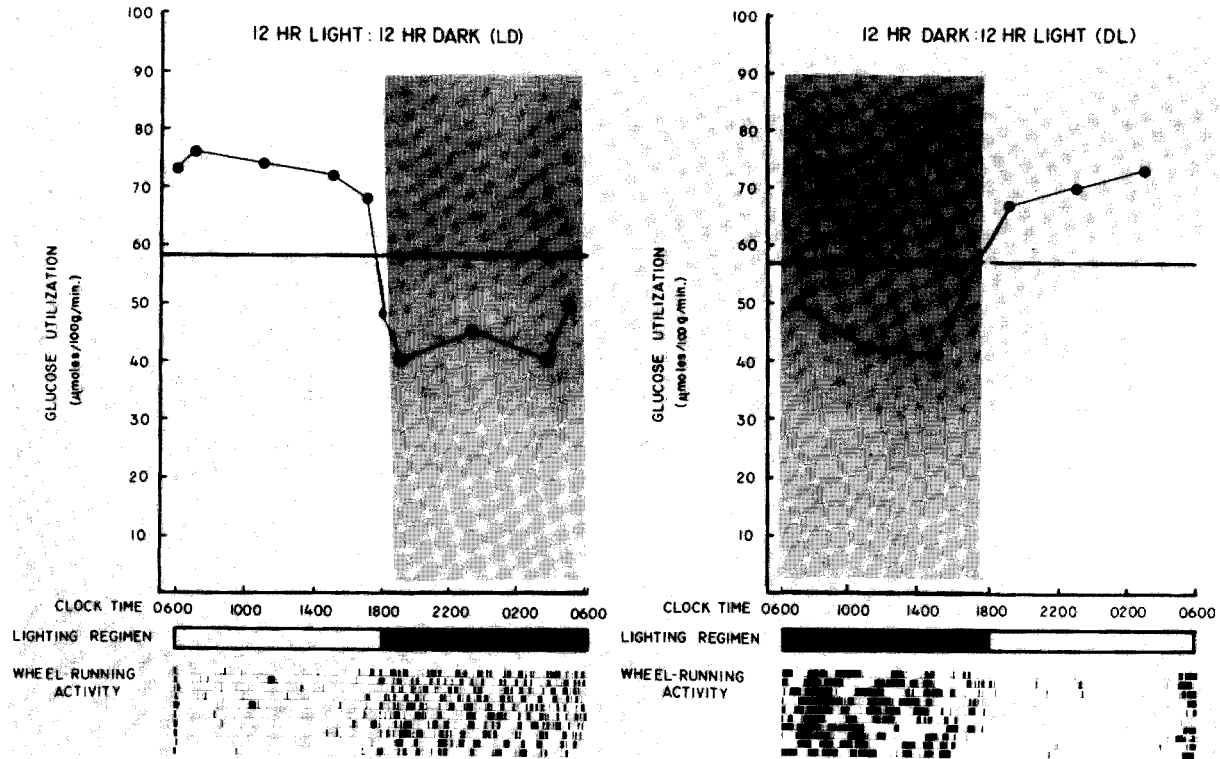


**Figure 11.** Circadian rhythms in glucose utilization in suprachiasmatic nucleus in the rat. *Left panel*, animals entrained to 12 hours of light during day and 12 hours of darkness during night. *Right panel*, animals entrained to opposite light-dark regimen. [Schwartz et al., 1980]

a role in the organization of circadian rhythms in the central nervous system.

Much of our knowledge of neurophysiology has been derived from studies of the electrical activity of the nervous system. Indeed, from the heavy emphasis that has been placed on electrophysiology, one might gather that the brain is really an electric organ rather than a chemical one that functions mainly by the release of chemical transmitters at synapses. Nevertheless, electrical activity is unquestionably fundamental to the process of conduction, and it is appropriate to inquire how the local metabolic activities revealed by the [ $^{14}\text{C}$ ]deoxyglucose method are related to the electrical activity of the nervous system. This question is currently being examined by Yarowsky and his coworkers (1979) in the superior cervical ganglion of the rat. The advantage of this structure is that its preganglionic input and postganglionic output can be isolated and electrically stimulated and/or monitored *in vivo*. The results thus far indicate a clear relationship between electrical input to the ganglion and its metabolic activity. In normal conscious rats the ganglion's rate of glucose utilization equals approximately 35  $\mu\text{moles}/100\text{ g}/\text{min}$ . This rate is markedly depressed by anesthesia or denervation and enhanced by electrical stimulation of the afferent nerves. The metabolic activation is frequency-dependent in the range of 5 to 15 Hz, increasing linearly in magnitude with increasing frequency of the stimulation (Figure 12). Similar effects of electrical stimulation on the oxygen and glucose consumption of the excised ganglion studied *in vitro* have been observed (Larrabee, 1958; Horowicz and Larrabee, 1958; Friedli, 1977). Recent studies have also shown that antidromic stimulation of the postganglionic efferent pathways from the ganglion has similar effects; stimulation of the external carotid nerve antidromically activates glucose utilization in the region of distribution of the cell bodies of this efferent pathway, indicating that not only the preganglionic axonal terminals are metabolically activated, but the postganglionic cell bodies as well (Yarowsky et al., 1980). As in the neurohypophysial pathway (Mata et al., 1980), the effects of electrical stimulation on energy metabolism in the superior cervical ganglion are probably due to the ionic currents associated with the spike activity and the consequent activation of the  $\text{Na}^+$ ,  $\text{K}^+$ -ATPase activity to restore the ionic gradients. Electrical stimulation of the afferents to sympathetic ganglia have been shown to increase extracellular  $\text{K}^+$  concentration (Friedli, 1977; Galvan et al., 1979). Each spike is normally associated with a sharp transient rise in extracellular  $\text{K}^+$  concentration, which then rapidly falls and transiently undershoots before returning to the normal level (Galvan et al., 1979); ouabain slows the decline in  $\text{K}^+$  con-

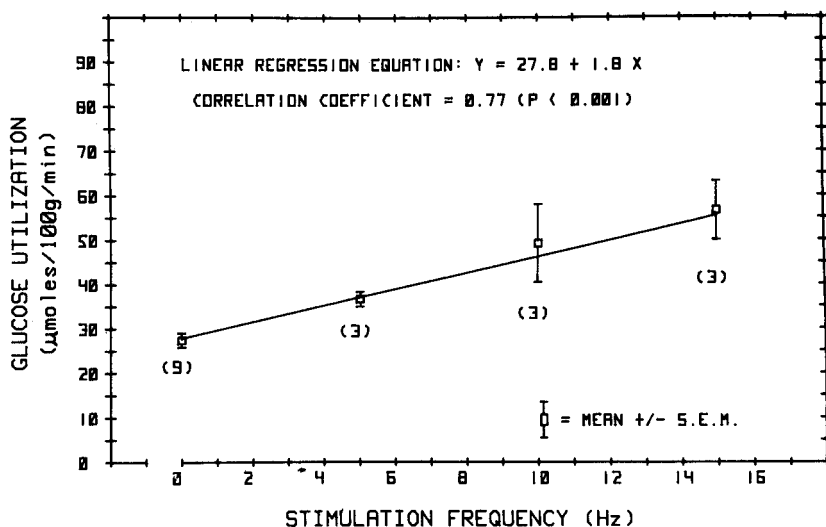


**Figure 12.**

Relationship between average glucose utilization in the superior cervical ganglion of the rat and the frequency of electrical stimulation of the cervical sympathetic trunk (i.e., preganglionic input). The animals were under urethane anesthesia. The cervical sympathetic trunk was transected, and the distal portion was stimulated with 0.3 to 0.4 msec monopolar pulses administered via a stimulation isolation unit at a maximum current of 500  $\mu\text{amps}$  and at the frequency indicated. [Yarowsky et al., 1979]

centration after the spike and eliminates the undershoot. Continuous stimulation at a frequency of 6 Hz produces a sustained increase in cellular  $\text{K}^+$  concentration (Galvan et al., 1979). It is likely that the increased extracellular  $\text{K}^+$  concentration and, almost certainly, increased intracellular  $\text{Na}^+$  concentration activate the  $\text{Na}^+$ ,  $\text{K}^+$ -ATPase, which in turn leads to the increased glucose utilization.

### Pharmacological Applications

The ability of the deoxyglucose method to map the entire brain for localized regions of altered functional activity on the basis of changes in energy metabolism offers a potent tool to identify the neural sites of action of agents with neuropharmacological and psychopharmacological actions. It does not, however, discriminate between the direct and indirect effects of the drug. An entire pathway may be activated even though the direct action of the drug may be exerted only at the origin of the pathway. This is of advantage for relating behavioral effects to central actions, but it is a disadvantage if the goal is to identify the primary site of action of the drug. To discriminate between direct and indirect actions of a drug, the [ $^{14}\text{C}$ ]deoxy-

glucose method must be combined with selectively placed lesions in the CNS that interrupt afferent pathways to the structure in question. If the metabolic effect of the drug then remains, then it is due to direct action; if lost, the effect is likely to be indirect and mediated via the interrupted pathway. Nevertheless, the method has proved to be useful in a number of pharmacological studies.

#### *Effects of $\gamma$ -Butyrolactone*

$\gamma$ -Hydroxybutyrate and  $\gamma$ -butyrolactone, which is hydrolyzed to  $\gamma$ -hydroxybutyrate in plasma, produce trance-like behavioral states associated with marked suppression of electroencephalographic activity (Roth and Giarman, 1966). These effects are reversible, and these drugs have been used clinically as anesthetic adjuvants. There is evidence that these agents lower neuronal activity in the nigrostriatal pathway and may act by inhibition of dopaminergic synapses (Roth, 1976). Studies in rats with the [ $^{14}\text{C}$ ]deoxyglucose technique have demonstrated that  $\gamma$ -butyrolactone produces profound dose-dependent reductions of glucose utilization throughout the brain (Wolfson et al., 1977). At the highest doses studied, 600 mg/kg of body weight, glucose utilization was reduced by approximately 75% in gray matter and 33% in white matter, but there was no obvious further specificity with respect to the local cerebral structures affected. The reversibility of the effects and the magnitude and diffuseness of the depression of cerebral metabolic rate suggest that this drug might be considered as a chemical substitute for hypothermia in conditions in which profound reversible reduction of cerebral metabolism is desired.

#### *Effects of D-Lysergic Acid Diethylamide*

The effects of the potent psychotomimetic agent, D-lysergic acid diethylamide, have been examined in the rat (Shinohara et al., 1976). In doses of 12.5 to 125  $\mu\text{g}/\text{kg}$ , it caused dose-dependent reductions in glucose utilization in a number of cerebral structures. With increasing dosage, more structures were affected and to a greater degree. There was no pattern in the distribution of the effects, at least none discernible at the present level of resolution, that might contribute to the understanding of the drug's psychotomimetic actions.

#### *Effects of Morphine Addiction and Withdrawal*

Acute morphine administration depresses glucose utilization in many areas of the brain, but the specific effects of morphine could not be distinguished from those of the hypercapnia produced by the associated respiratory depression (Sakurada et al., 1976). In contrast, morphine addiction, produced within 24 hours by a single subcutaneous in-

jection of 150 mg/kg of morphine base in an oil emulsion, reduces glucose utilization in a large number of gray structures in the absence of changes in arterial  $p\text{CO}_2$ . White matter appears to be unaffected. Naloxone (1 mg/kg subcutaneously) reduces glucose utilization in a number of structures when administered to normal rats, but when given to the morphine-addicted animals produces an acute withdrawal syndrome and reverses the reductions of glucose utilization in several structures, most strikingly in the habenula (Sakurada et al., 1976).

### *Pharmacological Studies of Dopaminergic Systems*

The most extensive applications of the deoxyglucose method to pharmacology have been in studies of dopaminergic systems. Ascending dopaminergic pathways appear to have a potent influence on glucose utilization in the forebrain of rats. Electrolytic lesions placed unilaterally in the lateral hypothalamus or pars compacta of the substantia nigra caused marked ipsilateral reductions of glucose metabolism in numerous forebrain structures rostral to the lesion, particularly the frontal cerebral cortex, caudate-putamen, and parts of the thalamus (Schwartz et al., 1976; Schwartz, 1978). Similar lesions in the locus coeruleus had no such effects.

Enhancement of dopaminergic synaptic activity by administration of the agonist of dopamine, apomorphine (Brown and Wolfson, 1978), or of amphetamine (Wechsler et al., 1979), which stimulates release of dopamine at the synapse, produces marked increases in glucose consumption in some of the components of the extrapyramidal system known or suspected to contain dopamine-receptive cells. With both drugs, the greatest increases noted were in the zona reticulata of the substantia nigra and the subthalamic nucleus. Surprisingly, none of the components of the dopaminergic mesolimbic system appeared to be affected.

The studies with amphetamine (Wechsler et al., 1979) were carried out with the fully quantitative [ $^{14}\text{C}$ ]deoxyglucose method. The results in Table 5 illustrate the comprehensiveness with which this method surveys the entire brain for sites of altered activity due to actions of the drug. It also allows for quantitative comparison of the relative potencies of related drugs. For example, in Table 5, the comparative effects of d-amphetamine and the less potent dopaminergic agent, l-amphetamine, are compared; the quantitative results clearly reveal that the effects of l-amphetamine on local cerebral glucose utilization are more limited in distribution and of less magnitude than those of d-amphetamine. Indeed, in similar quantitative studies with apomorphine, McCulloch and colleagues (1979, 1980a) have been able to generate complete dose-response curves for the effects of

the drug on the rates of glucose utilization in various components of dopaminergic systems. They have also demonstrated metabolically the development of supersensitivity to apomorphine in rats maintained chronically on the dopamine antagonist, haloperidol.\* In the course of these studies with apomorphine, McCulloch and coworkers (1980b) obtained evidence of a retinal dopaminergic system that projects specifically to the superficial layer of the superior colliculus in the rat. Apomorphine administration activated metabolism in the superficial layer of the superior colliculus, as well as in other structures, but the effect in the superficial layer was prevented by prior enucleation (Figure 13: see color insert). Miyaoka† subsequently observed that intraocular administration of minute amounts of apomorphine caused increased glucose utilization only in the superficial layer of the superior colliculus of the contralateral side.

#### *Effects of $\alpha$ - and $\beta$ -Adrenergic Blocking Agents*

Savaki and coworkers (1978) have studied the effects of the  $\alpha$ -adrenergic blocking agent, phentolamine, and the  $\beta$ -adrenergic blocking agent, propranolol. Both drugs produce widespread dose-dependent depressions of glucose utilization throughout the brain but exhibit particularly striking and opposite effects in the complete auditory pathway from the cochlear nucleus to the auditory cortex. Propranolol markedly depressed and phentolamine markedly enhanced glucose utilization in this pathway. The functional significance of these effects is unknown, but they seem to correlate with corresponding effects on the electrophysiological responsiveness of this sensory system. Propranolol depresses and phentolamine enhances the amplitude of all components of evoked auditory responses.††

#### **Pathophysiological Applications**

The application of the DG method to the study of pathological states has been limited because of uncertainties about the values for the lumped and rate constants to be used. There are, however, pathophysiological states in which there is no structural damage to the tissue, and the standard values of the constants can be used. Several of these conditions have been and are continuing to be studied by the [ $^{14}\text{C}$ ] deoxyglucose technique, both qualitatively and quantitatively.

\*J. McCulloch, H.E. Savaki, A. Pert, W. Bunney, and L. Sokoloff, unpublished observations.

†M. Miyaoka, unpublished observations.

††T. Furlow and J. Hallenbeck, personal communication.

**Table 5**

Effects of d-Amphetamine and l-Amphetamine on Local Cerebral Glucose Utilization in the Conscious Rat† [Wechsler et al., 1979]

Structure	Control	d-Amphetamine	l-Amphetamine
<b>Gray matter</b>			
Visual cortex	102 ± 8	135 ± 11*	105 ± 8
Auditory cortex	160 ± 11	162 ± 6	141 ± 6
Parietal cortex	109 ± 9	125 ± 10	116 ± 4
Sensory-motor cortex	118 ± 8	139 ± 9	111 ± 4
Olfactory cortex	100 ± 6	93 ± 5	94 ± 3
Frontal cortex	109 ± 10	130 ± 8	105 ± 4
Prefrontal cortex	146 ± 10	166 ± 7	154 ± 4
Thalamus – lateral nucleus	97 ± 5	114 ± 8	117 ± 6
– ventral nucleus	85 ± 7	108 ± 6*	96 ± 4
– habenula	118 ± 10	71 ± 5**	82 ± 2**
– dorsomedial nucleus	92 ± 6	111 ± 8	106 ± 6
Medial geniculate	116 ± 5	119 ± 4	116 ± 4
Lateral geniculate	79 ± 5	88 ± 5	84 ± 4
Hypothalamus	54 ± 5	56 ± 3	52 ± 3
– suprachiasmatic nucleus	94 ± 4	75 ± 4**	67 ± 1**
– mammillary body	117 ± 8	134 ± 5	142 ± 5*
Lateral olfactory nucleus §	92 ± 6	95 ± 5	99 ± 6
A <sub>13</sub>	71 ± 4	91 ± 4**	81 ± 4
Hippocampus – Ammon's horn	79 ± 5	73 ± 2	81 ± 6
– dentate gyrus	60 ± 4	55 ± 3	67 ± 7
Amygdala	46 ± 3	46 ± 3	44 ± 2
Septal nucleus	56 ± 3	55 ± 2	54 ± 3
Caudate nucleus	109 ± 5	132 ± 8*	127 ± 3*
Nucleus accumbens	76 ± 5	80 ± 3	78 ± 3
Globus pallidus	53 ± 3	64 ± 2*	65 ± 3*
Subthalamic nucleus	89 ± 6	149 ± 10**	107 ± 2
Substantia nigra – zona reticulata	58 ± 2	105 ± 4**	72 ± 4
– zona compacta	65 ± 4	88 ± 6**	72 ± 3
Red nucleus	76 ± 5	94 ± 5*	86 ± 2
Vestibular nucleus	121 ± 11	137 ± 5	130 ± 4
Cochlear nucleus	139 ± 6	126 ± 1	141 ± 5
Superior olivary nucleus	144 ± 4	143 ± 4	147 ± 6
Lateral lemniscus	107 ± 3	96 ± 5	98 ± 3
Inferior colliculus	193 ± 10	169 ± 5	150 ± 8**
Dorsal tegmental nucleus	109 ± 5	112 ± 7	122 ± 6
Superior colliculus	80 ± 5	89 ± 3	91 ± 3
Pontine gray	58 ± 4	65 ± 3	60 ± 1
Cerebellar flocculus	124 ± 10	146 ± 15	153 ± 10
Cerebellar hemispheres	55 ± 3	68 ± 6	64 ± 2

Table 5 (continued)

Structure	Control	d-Amphetamine	l-Amphetamine
Cerebellar nuclei	102 ± 4	105 ± 8	110 ± 3
<b>White matter</b>			
Corpus callosum	23 ± 3	24 ± 2	23 ± 1
Genu of corpus callosum	29 ± 2	30 ± 2	26 ± 2
Internal capsule	21 ± 1	24 ± 2	19 ± 2
Cerebellar white	28 ± 1	31 ± 2	31 ± 2

† All values are the means ± standard error of the mean for five animals.

\* Significant difference from the control at the  $p < 0.05$  level.

\*\* Significant difference from the control at the  $p < 0.01$  level.

§ It was not possible to correlate precisely this area on autoradiographs with a specific structure in the rat brain. It is, however, most likely the lateral olfactory nucleus.

### *Convulsive States*

The local injection of penicillin into the motor cortex produces focal seizures manifested in specific regions of the body contralaterally. The [ $^{14}\text{C}$ ]deoxyglucose method has been used to map the spread of seizure activity within the brain and to identify the structures with altered functional activity during the seizure. The partial results of one such experiment in the monkey are illustrated in Figure 5. Discrete regions of markedly increased glucose utilization, sometimes as much as 200%, are observed ipsilaterally in the motor cortex, basal ganglia, particularly the globus pallidus, thalamic nuclei, and contralaterally in the cerebellar cortex (Kennedy et al., 1975). Kato and coworkers (1980), Caviness and coworkers (1980), Hosokawa and collaborators (1980), and Caviness (1980) have carried out the most extensive studies of the propagation of the seizure activity in newborn and pubescent monkeys. The results indicate that the brain of the newborn monkey exhibits similar increases of glucose utilization in specific structures, but the pattern of distribution of the effects is less well defined than in the pubescent monkeys. Collins and colleagues (1976) have carried out similar studies in the rat with similar results but also obtained evidence on the basis of a local stimulation of glucose utilization of a "mirror focus" in the motor cortex contralateral to the side with the penicillin-induced epileptogenic focus.

Engel and coworkers (1978) have used the [ $^{14}\text{C}$ ]DG method to study seizures kindled in rats by daily electroconvulsive shocks. After a period of such treatment, the animals exhibit spontaneous seizures. Their results show marked increases in the limbic system, particularly the amygdala. The daily administration of the local anesthetic, lidocaine, kindles similar seizures in rats; Post and colleagues (1979) have

obtained similar results in such seizures, with particularly pronounced increases in glucose utilization in the amygdala, hippocampus, and the entorhinal cortex.

#### *Spreading Cortical Depression*

Shinohara and coworkers (1979) studied the effects of local applications of KCl on the dura overlying the parietal cortex of conscious rats or directly on the pial surface of the parietal cortex of anesthetized rats, in order to determine if  $K^+$  stimulates cerebral metabolism in vivo as it is well known to do in vitro. The results demonstrate a marked increase in cerebral cortical glucose utilization in response to the application of KCl; NaCl has no such effect (Figure 14). Such application of KCl, however, also produces the phenomenon of spreading cortical depression. This condition is characterized by a spread of transient, intense neuronal activity followed by membrane depolarization, electrical depression, and a negative shift in the cortical DC potential in all directions from the site of initiation at a rate of 2 to 5 mm/min. The depressed cortex also exhibits a number of chemical changes, including an increase in extracellular  $K^+$ , lost, presumably, from the cells. At the same time that the cortical glucose utilization is increased, most subcortical structures that are functionally connected to the depressed cortex exhibit decreased rates of glucose utilization. During recovery from the spreading cortical depression, the glucose utilization in the cortex is still increased, but it is distributed in columns oriented perpendicularly through the cortex. This columnar arrangement may reflect the columnar functional and morphological arrangement of the cerebral cortex. It is likely that the increased glucose utilization in the cortex during spreading cortical depression is the consequence of the increased extracellular  $K^+$  and activation of the  $Na^+$ ,  $K^+$ -ATPase.

#### *Opening of Blood-Brain Barrier*

Unilateral opening of the blood-brain barrier in rats by unilateral carotid injection with a hyperosmotic mannitol solution leads to widely distributed discrete regions of intensely increased glucose utilization in the ipsilateral hemisphere (Pappius et al., 1979). These focal regions of hypermetabolism may reflect local regions of seizure activity. The prior administration of diazepam in most cases prevents the appearance of these areas of increased metabolism (Pappius et al., 1979), and electroencephalographic recordings under similar experimental conditions reveal evidence of seizure activity.\*

\*C. Fieschi, personal communication.

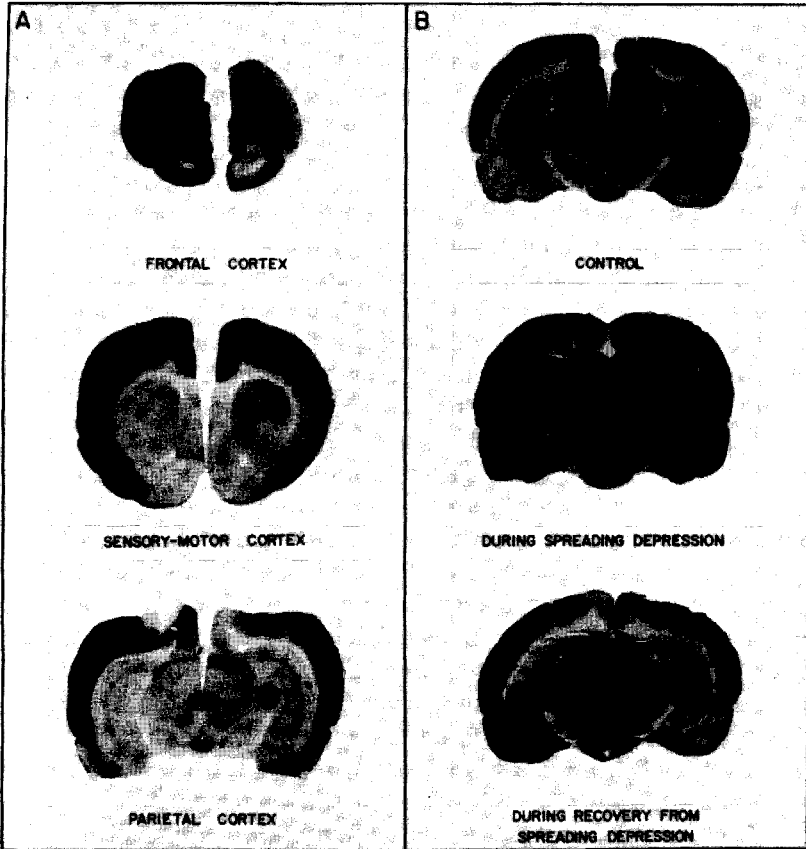


**Figure 14.**

Autoradiographs of sections of rat brains during spreading cortical depression and during recovery. The autoradiographs are pictorial representations of the relative rates of glucose utilization in various parts of the brain; the greater the density, the greater the rate of glucose utilization. The left sides of the brain are represented by the left hemispheres in the autoradiographs. In all the experiments illustrated, the control hemisphere was treated the same as the experimental side except that equivalent concentrations of NaCl rather than KCl were used. The NaCl did not lead to any detectable differences from hemispheres over which the skull was left intact and no NaCl was applied. A. Autoradiographs of sections of brain at different levels of cerebral cortex from a conscious rat during spreading cortical depression induced on the left side by application of 5M KCl to the intact dura overlying the left parietal cortex. The spreading depression was sustained by repeated applications of KCl at 15- to 20-minute intervals throughout the experimental period. B. Autoradiographs from sections of brain at the level of the parietal cortex from three animals under barbiturate anesthesia. The top section is from a normal anesthetized animal; the middle section is from an animal during unilateral spreading cortical depression induced and sustained by repeated applications of 80 mM KCl in artificial cerebrospinal fluid directly on the surface of the left parieto-occipital cortex. At the bottom is a comparable section from an animal studied immediately after the return of cortical d-c potential to normal after a single wave of spreading depression induced by a single application of 80 mM KCl to the parieto-occipital cortex of the left side. [Shinohara et al., 1979]

### *Hypoxemia*

Pulsinelli and Duffy (1979) have studied the effects of controlled hypoxemia on local cerebral glucose utilization by means of the qualitative [ $^{14}\text{C}$ ] deoxyglucose method. Hypoxemia was achieved by artificial ventilation of the animals with a mixture of  $\text{N}_2$ ,  $\text{N}_2\text{O}$ , and  $\text{O}_2$ , adjusted to maintain the arterial  $\text{pO}_2$  between 28 and 32 mm Hg. All the animals had had one common carotid artery ligated to limit the increase in cerebral blood flow and the amount of  $\text{O}_2$  delivered to the brain. Their autoradiographs provide striking evidence of marked and disparate changes in glucose utilization in the various structural components of the brain. The hemisphere ipsilateral to the carotid ligation was, not unexpectedly, more severely affected. The most striking effects were markedly higher increases in glucose utilization in white matter than in gray matter, presumably due to the Pasteur effect, and the appearance of transverse cortical columns of high activity alternating with columns of low activity. By studies with black plastic microspheres, Pulsinelli and Duffy were able to show that the cortical columns were anatomically related to penetrating cortical arteries, with the columns of high metabolic activity lying between the arteries.

Miyaoka and coworkers (1979b) have also studied the effects of moderate hypoxemia in normal, spontaneously breathing, conscious rats without carotid ligation. The hypoxemia was produced by lowering the  $\text{O}_2$  in the inspired air to approximately 7%. Although this procedure reduced arterial  $\text{pO}_2$  to approximately 30 mm Hg, the cerebral hypoxia was probably less than in the studies of Pulsinelli and Duffy (1979) because of the intact cerebral circulation. The animals remained fully conscious under these experimental conditions, although they appeared subdued and less active. The quantitative [ $^{14}\text{C}$ ] deoxyglucose method was employed, and rates of glucose utilization were determined. The results revealed many similarities to those of Pulsinelli and Duffy (1979). There was a complete redistribution of the local rates of glucose utilization from the normal pattern. Metabolism in white matter was markedly increased. Many areas showed decreased rates of metabolism. Columns were seen in the cerebral cortex, and the caudate nucleus exhibited a strange lace-like heterogeneity quite distinct from its normal homogeneity. Despite the widespread changes, however, overall average glucose utilization remained unchanged. These results are of relevance to the studies by Kety and Schmidt (1948b), who found in man that the breathing of 10%  $\text{O}_2$  produced a wide variety of mental symptoms without altering the average  $\text{O}_2$  consumption of the brain as a whole. The mental symptoms were probably the result of metabolic and functional

changes in specific regions of the brain, detectable only by methods like the deoxyglucose method that measure metabolic rate in the structural components of the brain.

### *Normal Aging*

Although, strictly speaking, aging is not a pathophysiological condition, many of its behavioral consequences are directly attributable to decrements in functions of the central nervous system (Birren et al., 1963). Normal human aging has been found to be associated with a decrease in average glucose utilization of the brain as a whole (Sokoloff, 1966). Smith and coworkers (1980) have employed the quantitative [ $^{14}\text{C}$ ]deoxyglucose method to study normal aging in Sprague-Dawley rats between 5 to 6 and 36 months of age. Their results show widespread but not homogeneous reductions of local cerebral glucose utilization with age. The sensory systems, particularly auditory and visual, are particularly severely affected. The caudate nucleus is metabolically depressed, and preliminary experiments indicate that it loses responsivity to dopamine agonists, such as apomorphine, with age.\* A striking effect was the loss of metabolically active neuropil in the cerebral cortex; Layer 4 is markedly decreased in metabolic activity and extent. Some of these changes may be related to specific functional disabilities that develop in old age.

## MICROSCOPIC RESOLUTION

The resolution of the present [ $^{14}\text{C}$ ]deoxyglucose method is at best approximately 100  $\mu\text{m}$ . The use of [ $^3\text{H}$ ]deoxyglucose does not greatly improve the resolution when the standard autoradiographic procedure is used. The limiting factor is the diffusion and migration of the water-soluble labeled compound in the tissue during the freezing of the brain and the cutting of the brain sections. Des Rosiers and Descarries (1978) have been working to extend the resolution of the method to the light and electron microscopic levels. They use [ $^3\text{H}$ ]deoxyglucose and dipping emulsion techniques. They have reported that fixation, postfixation, dehydration, and embedding of the brain by perfusion in situ results in negligible loss or migration of the label in the tissue. They can localize grain counts over individual cells or portions of them. Although the method is at present only qualitative, it is likely that it can eventually be adopted for quantitative use. An alternative promising approach to microscopic resolution is the use of freeze-substitution techniques (Ornberg et al., 1979; Sejnowski et al., 1980).

\*C. Smith and J. McCulloch, unpublished observations.

## THE [ $^{18}\text{F}$ ] FLUORODEOXYGLUCOSE TECHNIQUE

Because the deoxyglucose method requires the measurement of local concentrations of radioactivity in the individual components of the brain, it cannot be applied, as originally designed, to man. Recent developments in computerized emission tomography, however, have made it possible to measure local concentrations of labeled compounds in vivo in man. Emission tomography requires the use of  $\gamma$ -radiation, preferably annihilation  $\gamma$ -rays derived from positron emission. A positron-emitting derivative of deoxyglucose, 2- $^{18}\text{F}$  fluoro-2-deoxy-D-glucose has been synthesized and found to retain the necessary biochemical properties of 2-deoxyglucose (Reivich et al., 1979). The method has, therefore, been adapted for use in man with  $^{18}\text{F}$  fluorodeoxyglucose and positron-emission tomography (Reivich et al., 1979; Phelps et al., 1979). The resolution of the method is still relatively limited, approximately 1 cm, but it is already proving to be useful in studies of the human visual system (Figure 15: see color insert) (Phelps et al., 1980) and of clinical conditions, such as focal epilepsy (Figure 16: see color insert) (Kuhl et al., 1979, 1980). This technique is of immense potential usefulness for studies of human local cerebral energy metabolism in normal states and in neurological and psychiatric disorders.

## CONCLUDING REMARKS

The deoxyglucose method provides the means to determine quantitatively the rates of glucose utilization simultaneously in all structural and functional components of the central nervous system and to display them pictorially superimposed on the anatomical structures in which they occur. Because of the close relationship between local functional activity and energy metabolism, the method makes it possible to identify all structures with increased or decreased functional activity in various physiological, pharmacological, and pathophysiological states. The images provided by the method do resemble histological sections of nervous tissue, and the method is, therefore, sometimes misconstrued to be a neuroanatomical method and contrasted with physiological methods, such as electrophysiological recording. This classification obscures the most significant and unique feature of the method. The images are not of structure but of a dynamic biochemical process, glucose utilization, which is as physiological as electrical activity. In most situations, changes in functional activity result in changes in energy metabolism, and the images can be used to visualize and identify the sites of altered activity. The images are, therefore, analogous to infra-red maps; they record quantitatively the rates of a kinetic process and display them pictorially exactly where they exist. The fact that they depict the anatomical structures is fortuitous; it indicates that the rates of glucose utilization are distributed according to structure, and specific functions in the nervous system are associated with specific anatomical structures. The deoxyglucose method represents, therefore, in a real sense, a new type of encephalography, metabolic encephalography. At the very least, it should serve as a valuable supplement to more conventional methods, such as electroencephalography. Because, however, it provides a new means to examine another aspect of function simultaneously in all parts of the brain, it is hoped that it and its derivative, the [ $^{18}\text{F}$ ] fluoro-deoxyglucose technique, will open new roads to the understanding of how the brain works in health and disease.

## BIBLIOGRAPHY

- Albers, R.W. (1967): Biochemical aspects of active transport. *Annu. Rev. Biochem.* 36: 727-756.
- Bachelard, H.S. (1971): Specificity and kinetic properties of monosaccharide uptake into guinea pig cerebral cortex in vitro. *J. Neurochem.* 18: 213-222.
- Batipps, M., Miyaoka, M., Shinohara, M., Sokoloff, L., and Kennedy, C. (1981): Comparative rates of local cerebral glucose utilization in the visual system of conscious albino and pigmented rats. *Neurology* 31: 58-62.
- Bidder, T.G. (1968): Hexose translocation across the blood-brain interface: configurational aspects. *J. Neurochem.* 15: 867-874.
- Birren, J.E., Butler, R.N., Greenhouse, S.W., Sokoloff, L., and Yarrow, M.R., eds. (1963): *Human Aging: A Biological and Behavioral Study*. Washington, D.C.: U.S. Government Printing Office, Public Health Service Publication No. 986.
- Brown, L. and Wolfson, L. (1978): Apomorphine increases glucose utilization in the substantia nigra, subthalamic nucleus, and corpus striatum of the rat. *Brain Res.* 148: 188-193.
- Caldwell, P.C. (1968): Factors governing movement and distribution of inorganic ions in nerve and muscle. *Physiol. Rev.* 48: 1-64.
- Caveness, W.F., (1969): Ontogeny of focal seizures. In: *Basic Mechanisms of the Epilepsies*. Jasper, H.H., Ward, A.A., and Pope, A., eds. Boston: Little, Brown and Co., pp. 517-534.
- Caveness, W.F., (1980): Appendix: tables of local cerebral glucose utilization in various experimental preparations. *Ann. Neuro.* 7: 230-237.
- Caveness, W.F., Dato, M., Malamut, B.L., Hosokawa, S., Wakisaka, S., and O'Neill, R.R. (1980): Propagation of focal motor seizures in the pubescent monkey. *Ann. Neurol.* 7: 213-221.
- Collins, R.C., Kennedy, C., Sokoloff, L., and Plum, F. (1976): Metabolic anatomy of focal motor seizures. *Arch. Neurol.* 33: 536-542.
- Des Rosiers, M.H. and Descarries, L. (1978): Adaptation de la méthode au désoxyglucose à l'échelle cellulaire: préparation histologique du système nerveux central en vue de la radioautographie à haute résolution. *C.R. Acad. Sci.* 287: 153-156.
- Des Rosiers, M.H., Sakurada, O., Jehle, J., Shinohara, M., Kennedy, C., and Sokoloff, L. (1978): Functional plasticity in the immature striate cortex of the monkey shown by the [<sup>14</sup>C]deoxyglucose method. *Science* 200: 447-449.
- Duffy, T.E., Cavazzuti, M., Gregoire, N.M., Cruz, N.F., Kennedy, C., and Sokoloff, L. (1979): Regional cerebral glucose metabolism in newborn beagle dogs. *Trans. Am. Soc. Neurochem.* 10: 171. (Abstr.)
- Durham, D., and Woolsey, T.A. (1977): Barrels and columnar cortical organization: evidence from 2-deoxyglucose (2-DG) experiments. *Brain Res.* 137: 169-174.
- Eklöf, B., Lassen, N.A., Nilsson, L., Norberg, K., and Siesjö, B.K. (1973): Blood flow and metabolic rate for oxygen in the cerebral cortex of the rat. *Acta Physiol. Scand.* 88: 587-589.
- Engel, J., Jr., Wolfson, L., and Brown, L. (1978): Anatomical correlates of electrical and behavioral events related to amygdaloid kindling. *Ann. Neurol.* 3: 538-544.
- Freygang, W.H., Jr. and Sokoloff, L. (1958): Quantitative measurement of regional circulation in the central nervous system by the use of radioactive inert gas. *Adv. Biol. Med. Phys.* 6: 263-279.
- Friedli, C. (1977): Kinetics of changes in pO<sub>2</sub> and extracellular potassium activity in stimulated rat sympathetic ganglia. In: *Oxygen Transport to Tissue*. (Advances in Experimental Medicine and Biology, Vol. III.) Silver, I.A., Erecinska, M., and Bicher, H.I., eds. New York: Plenum Press, pp. 747-754.

- Galvan, M., Ten Bruggencate, G., and Senekowitsch, R. (1979): The effects of neuronal stimulation and ouabain upon extracellular  $K^+$  and  $Ca^{2+}$  levels in rat isolated sympathetic ganglia. *Brain Res.* 160: 544-548.
- Gjedde, A., Caronna, J.J., Hindfelt, B., and Plum, F. (1975): Whole-brain blood flow and oxygen metabolism in the rat during nitrous oxide anesthesia. *Am. J. Physiol.* 229: 113-118.
- Gooch, C., Rasband, W., and Sokoloff, L. (1980): Computerized densitometry and color coding of [ $^{14}C$ ] deoxyglucose autoradiographs. *Ann. Neurol.* 7: 359-370.
- Hand, P.J. (1981): The 2-deoxyglucose method. In: *Methods in Contemporary Neuroanatomy: The Tracing of Central Nervous Pathways*. New York: Plenum Press. (In press)
- Hand, P.J., Greenberg, J.H., Miselis, R.R., Weller, W.L., and Reivich, M. (1978): A normal and altered cortical column: a quantitative and qualitative ( $^{14}C$ )-2 deoxyglucose (2DG) mapping study. In: *Neurosciences Abstracts, Vol. IV*. (Eighth Annual Meeting of the Society for Neuroscience, St. Louis, MO, Nov. 5-9, 1978.) P. 553.
- Hers, H.G. (1957): *Le Métabolisme du Fructose*. Bruxelles: Editions Arscia, p. 102.
- Horowicz, P. and Larrabee, M.G. (1958): Glucose consumption and lactate production in a mammalian sympathetic ganglion at rest and in activity. *J. Neurochem.* 2: 102-118.
- Hosokawa, S., Iguchi, T., Caveness, W.F., Kato, M., O'Neill, R.R., Wakisaka, S., and Malamut, B.L. (1980): Effects of manipulation of the sensorimotor system of focal motor seizures in the monkey. *Ann. Neurol.* 7: 222-229.
- Hubel, D.H. and Wiesel, T.N. (1968): Receptive fields and functional architecture of monkey striate cortex. *J. Physiol.* 195: 215-243.
- Hubel, D.H. and Wiesel, T.N. (1972): Laminar and columnar distribution of geniculocortical fibers in the Macaque monkey. *J. Comp. Neurol.* 146: 421-450.
- Hubel, D.H., Wiesel, T.N., and Stryker, M.P. (1978): Anatomical demonstration of orientation columns in macaque monkey. *J. Comp. Neurol.* 177: 361-380.
- Jarvis, C.D., Mishkin, M., Shinohara, M., Sakurada, O., Miyaoka, M., and Kennedy, C. (1978): Mapping the primate visual system with the [ $^{14}C$ ] 2-deoxyglucose technique. In: *Neurosciences Abstracts, Vol. IV*. (Eighth Annual Meeting of The Society for Neuroscience, St. Louis, MO, Nov. 5-9, 1978.) P. 632.
- Kato, M., Malamut, B.L., Caveness, W.F., Hosokawa, S., Wakisaka, S., and O'Neill, R.R. (1980): Local cerebral glucose utilization in newborn and pubescent monkeys during focal motor seizures. *Ann. Neurol.* 7: 204-212.
- Kennedy, C., Des Rosiers, M., Jehle, J.W., Reivich, M., Sharp, F., and Sokoloff, L. (1975): Mapping of functional neural pathways by autoradiographic survey of local metabolic rate with [ $^{14}C$ ] deoxyglucose. *Science* 187: 850-853.
- Kennedy, C., Des Rosiers, M.H., Sakurada, O., Shinohara, M., Reivich, M., Jehle, J.W., and Sokoloff, L. (1976): Metabolic mapping of the primary visual system of the monkey by means of the autoradiographic [ $^{14}C$ ] deoxyglucose technique. *Proc. Nat. Acad. Sci.* 73: 4230-4234.
- Kennedy, C., Miyaoka, M., Suda, S., Macko, K., Jarvis, C., Mishkin, M., and Sokoloff, L. (1980): Local metabolic responses in brain accompanying motor activity. *Trans. Am. Neurol. Assoc.* (In press)
- Kennedy, C., Sakurada, O., Shinohara, M., Jehle, J., and Sokoloff, L. (1978): Local cerebral glucose utilization in the normal conscious Macaque monkey. *Ann. Neurol.* 4: 293-301.
- Kety, S.S. (1950): Circulation and metabolism of the human brain in health and disease. *Am. J. Med.* 8: 205-217.
- Kety, S.S. (1957): The general metabolism of the brain *in vivo*. In: *Metabolism of the Nervous System*. Richter, D., ed. London: Pergamon Press, pp. 221-237.
- Kety, S.S. (1960): Measurement of local blood flow by the exchange of an inert, diffusible substance. In: *Methods in Medical Research, Vol. VIII*. Bruner, D., ed., Chicago: Year Book Publishers, pp. 223-227.

- Kety, S.S. and Schmidt, C.F. (1948a): The nitrous oxide method for the quantitative determination of cerebral blood flow in man: theory, procedure, and normal values. *J. Clin. Invest.* 27: 476-483.
- Kety, S.S. and Schmidt, C.F. (1948b): Effects of altered arterial tensions of carbon dioxide and oxygen on cerebral blood flow and cerebral oxygen consumption of normal young men. *J. Clin. Invest.* 27: 484-492.
- Kuhl, D., Engel, J., Phelps, M., and Selin, C. (1979): Patterns of local cerebral metabolism and perfusion in partial epilepsy by emission computed tomography of  $^{18}\text{F}$ -fluorodeoxyglucose and  $^{13}\text{N}$ -ammonia. *Acta Neurol. Scand. Suppl.* (72) 538-539.
- Kuhl, D.E., Engel, J., Jr., Phelps, M.E., and Selin, C. (1980): Epileptic patterns of local cerebral metabolism and perfusion in humans determined by emission-computed tomography of  $^{18}\text{F}$ FDG and  $^{13}\text{NH}_3$ . *Ann. Neurol.* 8: 348-360.
- Landau, W.M., Freygang, W.H., Jr., Rowland, L.P., Sokoloff, L., and Kety, S.S. (1955): The local circulation of the living brain; values in the unanesthetized and anesthetized cat. *Trans. Am. Neurol. Assoc.* 80: 125-129.
- Larrabee, M.G. (1958): Oxygen consumption of excised sympathetic ganglia at rest and in activity. *J. Neurochem.* 2: 81-101.
- Lashley, K.S. (1934): The mechanism of vision. VII. The projection of the retina upon the primary optic centers of the rat. *J. Comp. Neurol.* 59: 341-373.
- Lassen, N.A. (1959): Cerebral blood flow and oxygen consumption in man. *Physiol. Rev.* 39: 183-238.
- Lassen, N.A. and Munck, O. (1955): The cerebral blood flow in man determined by the use of radioactive krypton. *Acta Physiol. Scand.* 33: 30-49.
- McCulloch, J., Savaki, H.E., McCulloch, M.C., and Sokoloff, L. (1979): Specific distribution of metabolic alterations in cerebral cortex following apomorphine administration. *Nature* 282: 303-305.
- McCulloch, J., Savaki, H.E., and Sokoloff, L. (1980a): Influence of dopaminergic systems on the lateral habenular nucleus of the rat. *Brain Res.* 194: 117-124.
- McCulloch, J., Savaki, H.E., McCulloch, M.C., and Sokoloff, L. (1980b): Retina-dependent activation by apomorphine of metabolic activity in the superficial layer of the superior colliculus. *Science* 207: 313-315.
- Mata, M., Fink, D.J., Gainer, H., Smith, C.B., Davidsen, L., Savaki, H., Schwartz, W.J., and Sokoloff, L. (1980): Activity-dependent energy metabolism in rat posterior pituitary reflects sodium pump activity. *J. Neurochem.* 34: 213-215.
- Miyaoka, M., Shinohara, M., Batipps, M., Pettigrew, K.D., Kennedy, C., and Sokoloff, L. (1979a): The relationship between the intensity of the stimulus and the metabolic response in the visual system of the rat. *Acta Neurol. Scand. Suppl.* (72) 60: 16-17.
- Miyaoka, M., Shinohara, M., Kennedy, C., and Sokoloff, L. (1979b): Alterations in local cerebral glucose utilization (LCGU) in rat brain during hypoxemia. *Trans. Am. Neurol. Assoc.* (In press)
- Montero, V.M. and Guillery, R.W. (1968): Degeneration in the dorsal lateral geniculate nucleus of the rat following interruption of the retinal or cortical connections. *J. Comp. Neurol.* 134: 211-242.
- Nordmann, J.J. (1977): Ultrastructural morphometry of the rat neurohypophysis. *J. Anat.* 123: 213-218.
- Oldendorf, W.H. (1971): Brain uptake of radiolabeled amino acids, amines, and hexoses after arterial injection. *Am. J. Physiol.* 221: 1629-1638.
- Ornberg, R.L., Neale, E.A., Smith, C.B., Yarowsky, P., Bowers, L.M. (1979): Radioautographic localization of glucose utilization by neurons in culture. *J. Cell Biol.* 83: 142. (Abstr.)
- Pappius, H.M., Savaki, H.E., Fieschi, C., Rapoport, S.I., and Sokoloff, L. (1979): Osmotic

- opening of the blood-brain barrier and local cerebral glucose utilization. *Ann. Neurol.* 5: 211-219.
- Phelps, M.E., Huang, S.C., Hoffman, E.J., Selin, C., Sokoloff, L., and Kuhl, D.E. (1979): Tomographic measurement of local cerebral glucose metabolic rate in humans with (F-18)-2-fluoro-2-deoxy-d-glucose: validation of method. *Ann Neurol.* 6:371-388.
- Phelps, M.E., Mazziotta, J.C. and Kuhl, D.E. (1980): Metabolic mapping of the brain's response to visual stimulation: studies in man. *Science* (In press)
- Plum, F., Gjedde, A., and Samson, F.E. (1976): Neuroanatomical functional mapping by the radioactive 2-deoxy-D-glucose method. *Neurosciences Res. Prog. Bull.* 14: 457-518.
- Post, R.M., Kennedy, C., Shinohara, M., Squillance, K., Miyaoka, M., Suda, S., Ingvar, D.H., and Sokoloff, L. (1979): Local cerebral glucose utilization in lidocaine-kindled seizures. *In: Neuroscience Abstracts, Vol. V.* (Ninth Annual Meeting of the Society for Neurosciences, Atlanta, GA, Nov. 2-6, 1979.) P. 196.
- Pulsinelli, W.A. and Duffy, T.E. (1979): Local cerebral glucose metabolism during controlled hypoxemia in rats. *Science* 204: 626-629.
- Rakic, P. (1976): Prenatal genesis of connections subserving ocular dominance in the rhesus monkey. *Nature* 261: 467-471.
- Reivich, M., Jehle, J., Sokoloff, L., and Kety, S.S. (1969): Measurement of regional cerebral blood flow with antipyrine-<sup>14</sup>C in awake cats. *J. Appl. Physiol.* 27: 296-300.
- Reivich, M., Kuhl, D., Wolf, A., Greenberg, J., Phelps, M., Ido, T., Cassella, V., Fowler, J., Hoffman, E., Alavi, A., Som, P., and Sokoloff, L. (1979): The [<sup>18</sup>F] fluoro-deoxyglucose method for the measurement of local cerebral glucose utilization in man. *Circ. Res.* 44: 127-137.
- Roth, R.H. (1976): Striatal dopamine and gamma-hydroxybutyrate. *Pharmacol. Ther.* 2: 71-88.
- Roth, R.H. and Giarman, J.J. (1966):  $\gamma$ -Butyrolactone and  $\gamma$ -hydroxybutyric acid. - I. Distribution and metabolism. *Biochem. Pharmacol.* 15: 1333-1348.
- Sacks, W. (1957): Cerebral metabolism of isotopic glucose in normal human subjects. *J. Appl. Physiol.* 10: 37-44.
- Sakurada, O., Shinohara, M., Klee, W.A., Kennedy, C., and Sokoloff, L. (1976): Local cerebral glucose utilization following acute or chronic morphine administration and withdrawal. *In: Neuroscience Abstracts, Vol. II, Part I.* (Sixth Annual Meeting of the Society for Neuroscience, Toronto, Canada, Nov. 7-11, 1976.) P. 613.
- Savaki, H.E., Kadekaro, M., Jehle, J., and Sokoloff, L. (1978):  $\alpha$ - and  $\beta$ -adrenoreceptor blockers have opposite effects on energy metabolism of the central auditory system. *Nature* 276: 521-523.
- Scheinberg, P. and Stead, E.A., Jr. (1949): The cerebral blood flow in male subjects as measured by the nitrous oxide technique. Normal values for blood flow, oxygen utilization, and peripheral resistance, with observations on the effect of tilting and anxiety. *J. Clin. Invest.* 28: 1163-1171.
- Schwartz, W.J. (1978): A role for the dopaminergic nigrostriatal bundle in the pathogenesis of altered brain glucose consumption after lateral hypothalamic lesions. Evidence using the <sup>14</sup>C-labeled deoxyglucose technique. *Brain Res.* 158: 129-147.
- Schwartz, W.J., Davidsen, L.C., and Smith, C.B. (1980): *In vivo* metabolic activity of a putative circadian oscillator, the rat suprachiasmatic nucleus. *J. Comp. Neurol.* 189: 157-167.
- Schwartz, W.J. and Gainer, H. (1977): Suprachiasmatic nucleus: use of <sup>14</sup>C-labeled deoxyglucose uptake as a functional marker. *Science* 197: 1089-1091.
- Schwartz, W.J., Sharp, F.R., Gunn, R.H., and Everts, E.V. (1976): Lesions of ascending dopaminergic pathways decrease forebrain glucose uptake. *Nature* 261: 155-157.
- Schwartz, W.J., Smith, C.B., Davidsen, L., Savaki, H., Sokoloff, L., Mata, M., Fink, D.J., and

- Gainer, H. (1979): Metabolic mapping of functional activity in the hypothalamo-neurohypophysial system of the rat. *Science* 205: 723-725.
- Sejnowski, T.J., Reingold, S.C., Kelley, D.B., and Gelperin, A. (1980): Localization of [<sup>3</sup>H]-2-deoxyglucose in single molluscan neurones. *Nature* 287: 449-451.
- Sharp, F.R., Kauer, J.S., and Shepherd, G.M. (1975): Local sites of activity-related glucose metabolism in rat olfactory bulb during olfactory stimulation. *Brain Res.* 98: 596-600.
- Shinohara, M., Dollinger, B., Brown, G., Rapoport, S., and Sokoloff, L. (1979): Cerebral glucose utilization: local changes during and after recovery from spreading cortical depression. *Science* 20: 188-190.
- Shinohara, M., Sakurada, O., Jehle, J., and Sokoloff, L. (1976): Effects of D-lysergic acid diethylamide on local cerebral glucose utilization in the rat. In: *Neuroscience Abstracts, Vol. II, Part 1.* (Sixth Annual Meeting of the Society for Neuroscience, Toronto, Canada, Nov. 7-11, 1976.) P. 615.
- Silverman, M.S., Hendrickson, A.E., and Clopton, B.M. (1977): Mapping of the tonotopic organization of the auditory system by uptake of radioactive metabolites. In: *Neuroscience Abstracts, Vol. III.* (Seventh Annual Meeting of the Society for Neuroscience, Anaheim, CA, Nov. 6-10, 1977.) P. 11.
- Smith, C.B., Goochee, C., Rapoport, S.I., and Sokoloff, L. (1980): Effects of ageing on local rates of cerebral glucose utilization in the rat. *Brain* 103: 351-365.
- Sokoloff, L. (1960): Metabolism of the central nervous system *in vivo*. In: *Handbook of Physiology. Section 1: Neurophysiology, Vol. III.* Field, J., Magoun, H.W., and Hall, V.E. eds. Washington, D.C.: American Physiological Society, pp. 1843-1864.
- Sokoloff, L. (1966): Cerebral circulatory and metabolic changes associated with aging. *Res. Publ. Ass. Nerv. Ment. Dis.* 41: 237-254.
- Sokoloff, L. (1969): Cerebral circulation and behavior in man: strategy and findings. In: *Psychochemical Research in Man.* Mandell, A.J. and Mandell, M.P., eds. New York: Academic Press, pp. 237-252.
- Sokoloff, L. (1976): Circulation and energy metabolism of the brain. In: *Basic Neurochemistry.* Second edition. Siegel, G.J., Albers, R.W., Katzman, R., and Agranoff, B.W., eds. Boston: Little, Brown and Co., pp. 388-413.
- Sokoloff, L. (1977): Relation between physiological function and energy metabolism in the central nervous system. *J. Neurochem.* 29: 13-26.
- Sokoloff, L. (1978): Mapping cerebral functional activity with radioactive deoxyglucose. *TINS* 1: 75-79.
- Sokoloff, L. (1979): The [<sup>14</sup>C]deoxyglucose method: four years later. *Acta Neurol. Scand. Suppl. (70)* 60: 640-649.
- Sokoloff, L., Reivich, M., Kennedy, C., Des Rosiers, M.H., Patlak, C.S., Pettigrew, K.D., Sakurada, O., and Shinohara, M. (1977): The [<sup>14</sup>C]deoxyglucose method for the measurement of local cerebral glucose utilization: theory, procedure, and normal values in the conscious and anesthetized albino rat. *J. Neurochem.* 28: 897-916.
- Sols, A. and Crane, R.K. (1954): Substrate specificity of brain hexokinase. *J. Biol. Chem.* 210: 581-595.
- Webster, W.R., Serviere, J., Batini, C., and LaPlante, S. (1978): Autoradiographic demonstration with 2-[<sup>14</sup>C]deoxyglucose of frequency selectivity in the auditory system of cats under conditions of functional activity. *Neurosci. Lett.* 10: 43-48.
- Wechsler, L.R., Savaki, H.E., and Sokoloff, L. (1979): Effects of d- and l-amphetamine on local cerebral glucose utilization in the conscious rat. *J. Neurochem.* 32: 15-22.
- Whittam, R. (1962): The dependence of the respiration of brain cortex on active cation transport. *Biochem. J.* 82: 205-212.
- Wiesel, T.N., Hubel, D.H., and Lam, D.M.K. (1974): Autoradiographic demonstration of ocular dominance columns in the monkey striate cortex by means of transneuronal trans-

port. *Brain Res.* 79: 273-279.

Wolfson, L.I., Sakurada, O., and Sokoloff, L. (1977): Effects of  $\gamma$ -butyrolactone on local cerebral glucose utilization in the rat. *J. Neurochem.* 29: 777-783.

Yarowsky, P.J., Jehle, J., Ingvar, D.H., and Sokoloff, L. (1979): Relationship between functional activity and glucose utilization in the rat superior cervical ganglion *in vivo*. *In: Neuroscience Abstracts, Vol. V.* (Ninth Annual Meeting of the Society for Neuroscience, Atlanta, GA, Nov. 2-6, 1979.) P. 421.

Yarowsky, P., Crane, A.M., and Sokoloff, L. (1980): Stimulation of neuronal glucose utilization by antidromic electrical stimulation in the superior cervical ganglion of the rat. *In: Neuroscience Abstracts, Vol. VI.* (Tenth Annual Meeting of the Society for Neuroscience.) P. 340.